4

Diffraction II: Intensities of Diffracted Beams

4–1 INTRODUCTION

As stated earlier, the positions of the atoms in the unit cell affect the intensities but not the directions of the diffracted beams. That this must be so may be seen by considering the two structures shown in Fig. 4–1. Both are orthorhombic with two atoms of the same kind per unit cell, but the one on the left is base-centered and the one on the right body-centered. Either is derivable from the other by a simple shift of one atom by the vector $\frac{1}{2}\mathbf{c}$.

Consider reflections from the (001) planes which are shown in profile in Fig. 4–2. For the base-centered lattice shown in (a), suppose that the Bragg law is satisfied for the particular values of λ and θ employed. This means that the path difference ABC between rays **1′** and **2′** is one wavelength, so that rays **1′** and **2′** are in phase and diffraction occurs in the direction shown. Similarly, in the body-centered lattice shown in (b), rays **1′** and **2′** are in phase, since their path difference ABC is one wavelength. However, in this case, there is another plane of atoms midway between the (001) planes, and the path difference DEF between rays **1′** and **3′** is exactly half of ABC, or one-half wavelength. Thus rays **1′** and **3′** are completely out of phase and annul each other. Similarly, ray **4′** from the next plane down (not shown) annuls ray **2′**, and so on throughout the crystal. There is no 001 reflection from the body-centered lattice.

This example shows how a simple rearrangement of atoms within the unit cell can eliminate a reflection completely. More generally, the intensity of a diffracted beam is changed, not necessarily to zero, by any change in atomic positions, and, conversely, we can determine atomic positions only by observations of diffracted intensities. To establish an exact relation between atom position and intensity is the main purpose of this chapter. The problem is complex because of the many variables involved, and we will have to proceed step by step: we will consider how x-rays are scattered first by a single electron, then by an atom, and finally by all the atoms in the unit cell. We will apply these results to the powder method of x-ray diffraction only, and, to obtain an expression for the intensity of a powder pattern line, we will have to consider a number of other factors which affect the way in which a crystalline powder diffracts x-rays.

4–2 SCATTERING BY AN ELECTRON

We have seen in Chap. 1 that an x-ray beam is an electromagnetic wave characterized by an electric field whose strength varies sinusoidally with time at any one

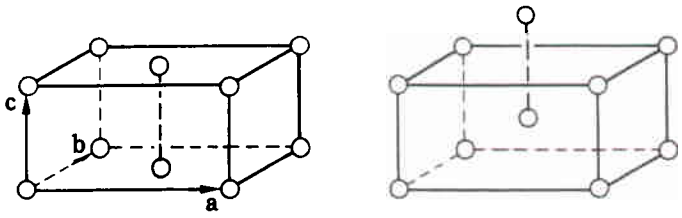

(a) (b)

Fig. 4–1 (a) Base-centered and (b) body-centered orthorhombic unit cells.

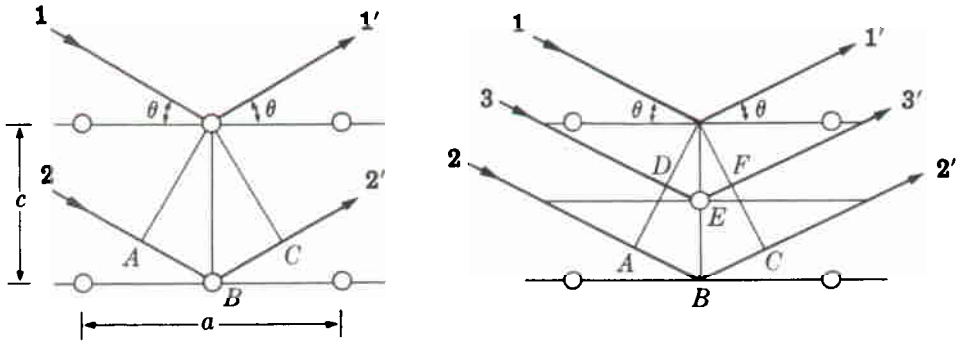

(a) (b)

Fig. 4–2 Diffraction from the (001) planes of (a) base-centered and (b) body-centered orthorhombic lattices.

point in the beam. Since an electric field exerts a force on a charged particle such as an electron, the oscillating electric field of an x-ray beam will set any electron it encounters into oscillatory motion about its mean position.

Now an accelerating or decelerating electron emits an electromagnetic wave. We have already seen an example of this phenomenon in the x-ray tube, where x-rays are emitted because of the rapid deceleration of the electrons striking the target. Similarly, an electron which has been set into oscillation by an x-ray beam is continuously accelerating and decelerating during its motion and therefore emits an electromagnetic wave. In this sense, an electron is said to *scatter* x-rays, the scattered beam being simply the beam radiated by the electron under the action of the incident beam. The scattered beam has the same wavelength and frequency as the incident beam and is said to be *coherent* with it, since there is a definite relationship between the phase of the scattered beam and that of the incident beam which produced it. (The phase change on scattering from an electron is $\lambda/2$. Because it is exactly the same for all the electrons in a crystal, it cancels out in any consideration of phase differences between rays scattered by different atoms, as in Fig. 3–2, and so does not affect the derivation of the Bragg law given in Sec. 3–2.)

Although x-rays are scattered in all directions by an electron, the intensity of the scattered beam depends on the angle of scattering, in a way which was first

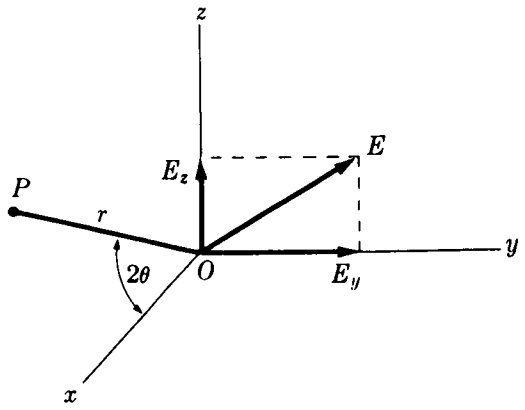

Fig. 4–3 Coherent scattering of x-rays by a single electron.

worked out by J. J. Thomson. He found that the intensity I of the beam scattered by a single electron of charge e coulombs (C) and mass m kg, at a distance r meters from the electron, is given by

$$I = I_0 \left(\frac{\mu_0}{4\pi}\right)^2 \left(\frac{e^4}{m^2 r^2}\right) \sin^2 \alpha = I_0 \frac{K}{r^2} \sin^2 \alpha \qquad (4\text{–}1)$$

where I_0 = intensity of the incident beam, $\mu_0 = 4\pi \times 10^{-7}$ m kg C^{-2}, K = constant, and α = angle between the scattering direction and the direction of acceleration of the electron. Suppose the incident beam is traveling in the direction Ox (Fig. 4–3) and encounters an electron at O. We wish to know the scattered intensity at P in the xz plane where OP is inclined at a scattering angle of 2θ to the incident beam. An unpolarized incident beam, such as that issuing from an x-ray tube, has its electric vector $\mathbf{E}$ in a random direction in the yz plane. This beam may be resolved into two plane-polarized components, having electric vectors $\mathbf{E}_y$ and $\mathbf{E}_z$ where

$$\mathbf{E}^2 = \mathbf{E}_y^2 + \mathbf{E}_z^2.$$

On the average, $\mathbf{E}_y$ will be equal to $\mathbf{E}_z$, since the direction of $\mathbf{E}$ is perfectly random. Therefore

$$\mathbf{E}_y^2 = \mathbf{E}_z^2 = \tfrac{1}{2}\mathbf{E}^2.$$

The intensity of these two components of the incident beam is proportional to the square of their electric vectors, since $\mathbf{E}$ measures the amplitude of the wave and the intensity of a wave is proportional to the square of its amplitude. Therefore

$$I_{0y} = I_{0z} = \tfrac{1}{2} I_0.$$

The y component of the incident beam accelerates the electron in the direction Oy. It therefore gives rise to a scattered beam whose intensity at P is found from Eq. (4–1) to be

$$I_{Py} = I_{0y} \frac{K}{r^2},$$

since $\alpha = \measuredangle yOP = \pi/2$. Similarly, the intensity of the scattered z component is given by

$$I_{Pz} = I_{0z} \frac{K}{r^2} \cos^2 2\theta,$$

since $\alpha = \pi/2 - 2\theta$. The total scattered intensity at P is obtained by summing the intensities of these two scattered components:

$$\begin{aligned} I_P &= I_{Py} + I_{Pz} \\ &= \frac{K}{r^2}(I_{0y} + I_{0z} \cos^2 2\theta) \\ &= \frac{K}{r^2}\left(\frac{I_0}{2} + \frac{I_0}{2} \cos^2 2\theta\right) \\ &= I_0 \frac{K}{r^2}\left(\frac{1 + \cos^2 2\theta}{2}\right). \end{aligned} \tag{4-2}$$

This is the Thomson equation for the scattering of an x-ray beam by a single electron. The intensity of the scattered beam is only a minute fraction of the intensity of the incident beam; the value of K is 7.94×10^{-30} m^2, so that I_P/I_0 is only 7.94×10^{-26} in the forward direction at 1 cm from the electron. The equation also shows that the scattered intensity decreases as the inverse square of the distance from the scattering electron, as one would expect, and that the scattered beam is stronger in forward or backward directions than in a direction at right angles to the incident beam.

The Thomson equation gives the absolute intensity (in ergs/sq cm/sec) of the scattered beam in terms of the absolute intensity of the incident beam. These absolute intensities are both difficult to measure and difficult to calculate, so it is fortunate that relative values are sufficient for our purposes in practically all diffraction problems. In most cases, all factors in Eq. (4–2) except the last are constant during the experiment and can be omitted. This last factor, $\frac{1}{2}(1 + \cos^2 2\theta)$, is called the *polarization factor*; this is a rather unfortunate term because, as we have just seen, this factor enters the equation simply because the incident beam is unpolarized. The polarization factor is common to all intensity calculations, and we will use it later in our equation for the intensity of a beam diffracted by a crystalline powder.

There is another and quite different way in which an electron can scatter x-rays, and that is manifested in the *Compton effect*. This effect, discovered by A. H. Compton in 1923, occurs whenever x-rays encounter loosely bound or free electrons and can be understood only by considering the incident beam not as a wave motion, but as a stream of x-ray quanta or photons, each of energy $h\nu_1$. When such a photon strikes a loosely bound electron, the collision is an elastic one like that of two billiard balls (Fig. 4–4). The electron is knocked aside and the photon is deviated through an angle 2θ. Since some of the energy of the incident photon is used in providing kinetic energy for the electron, the energy $h\nu_2$ of the photon after impact is less than its energy $h\nu_1$ before impact. The wavelength λ_2 of the

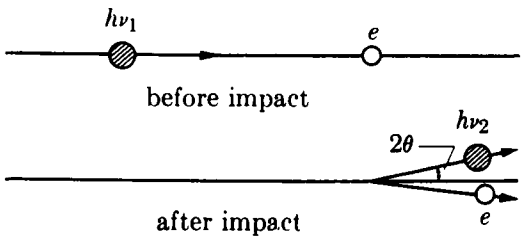

Fig. 4–4 Elastic collision of photon and electron (Compton effect).

scattered radiation is thus slightly greater than the wavelength λ_1 of the incident beam, the magnitude of the change being given by the equation

$$\Delta\lambda(\text{Å}) = \lambda_2 - \lambda_1 = 0.0486 \sin^2 \theta. \tag{4–3}$$

The increase in wavelength depends only on the scattering angle, and it varies from zero in the forward direction ($2\theta = 0$) to 0.05 Å in the extreme backward direction ($2\theta = 180°$).

Radiation so scattered is called *Compton modified radiation*, and, besides having its wavelength increased, it has the important characteristic that *its phase has no fixed relation to the phase of the incident beam.* For this reason it is also known as incoherent radiation. It cannot take part in diffraction because its phase is only randomly related to that of the incident beam and cannot therefore produce any interference effects. Compton modified scattering cannot be prevented, however, and it has the undesirable effect of darkening the background of diffraction patterns.

(It should be noted that the quantum theory can account for both the coherent and the incoherent scattering, whereas the wave theory is applicable only to the former. In terms of the quantum theory, coherent scattering occurs when an incident photon bounces off an electron which is so tightly bound that the electron receives no momentum from the impact. The scattered photon therefore has the same energy, and hence wavelength, as it had before.)

4–3 SCATTERING BY AN ATOM

When an x-ray beam encounters an atom, each electron in it scatters part of the radiation coherently in accordance with the Thomson equation. One might also expect the nucleus to take part in the coherent scattering, since it also bears a charge and should be capable of oscillating under the influence of the incident beam. However, the nucleus has an extremely large mass relative to that of the electron and cannot be made to oscillate to any appreciable extent; in fact, the Thomson equation shows that the intensity of coherent scattering is inversely proportional to the square of the mass of the scattering particle. The net effect is that coherent scattering by an atom is due only to the electrons contained in that atom.

The following question then arises: is the wave scattered by an atom simply the sum of the waves scattered by its component electrons? More precisely, does an atom of atomic number Z, i.e., an atom containing Z electrons, scatter a wave

whose amplitude is Z times the amplitude of the wave scattered by a single electron? The answer is yes, if the scattering is in the forward direction ($2\theta = 0$), because the waves scattered by all the electrons of the atom are then in phase and the amplitudes of all the scattered waves can be added directly.

This is not true for other directions of scattering. The fact that the electrons of an atom are situated at different points in space introduces differences in phase between the waves scattered by different electrons. Consider Fig. 4–5, in which, for simplicity, the electrons are shown as points arranged around the central nucleus. The waves scattered in the forward direction by electrons A and B are exactly in phase on a wave front such as XX', because each wave has traveled the same distance before and after scattering. The other scattered waves shown in the figure, however, have a path difference equal to $(CB - AD)$ and are thus somewhat out of phase along a wave front such as YY', the path difference being less than one wavelength. Partial interference occurs between the waves scattered by A and B, with the result that the net amplitude of the wave scattered in this direction is less than that of the wave scattered by the same electrons in the forward direction.

A quantity f, *the atomic scattering factor*, is used to describe the "efficiency" of scattering of a given atom in a given direction. It is defined as a ratio of amplitudes:

$$f = \frac{\text{amplitude of the wave scattered by an atom}}{\text{amplitude of the wave scattered by one electron}}.$$

From what has been said already, it is clear that $f = Z$ for any atom scattering in the forward direction. As θ increases, however, the waves scattered by individual electrons become more and more out of phase and f decreases. The atomic scattering factor depends also on the wavelength of the incident beam: at a fixed

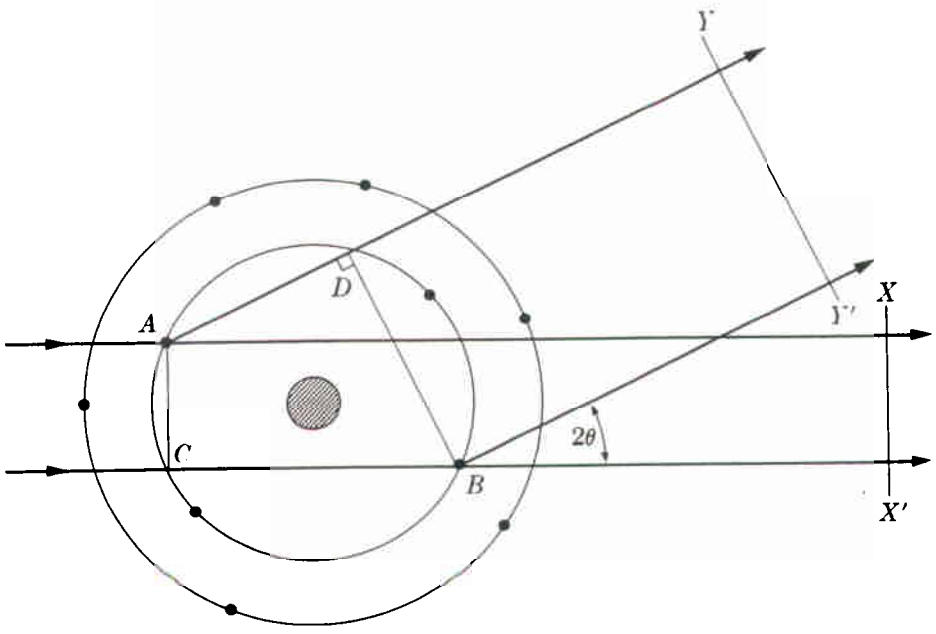

Fig. 4–5 X-ray scattering by an atom.

value of θ, f will be smaller the shorter the wavelength, since the path differences will be larger relative to the wavelength, leading to greater interference between the scattered beams. The actual calculation of f involves $\sin\theta$ rather than θ, so that the net effect is that f decreases as the quantity $(\sin\theta)/\lambda$ increases. The scattering factor f is sometimes called the *form factor*, because it depends on the way in which the electrons are distributed around the nucleus.

Calculated values of f for various atoms and various values of $(\sin\theta)/\lambda$ are tabulated in Appendix 12, and a curve showing the typical variation of f, in this case for copper, is given in Fig. 4–6. Note again that the curve begins at the atomic number of copper, 29, and decreases to very low values for scattering in the backward direction (θ near 90°) or for very short wavelengths. Since the intensity of a wave is proportional to the square of its amplitude, a curve of scattered intensity from an atom can be obtained simply by squaring the ordinates of a curve such as Fig. 4–6. (The resulting curve closely approximates the observed scattered intensity per atom of a monatomic gas, as shown in Fig. 3–18.)

Strictly, the scattering factors f tabulated in Appendix 12 apply only when the scattered radiation has a wavelength much shorter than that of an absorption edge of the scattering atom. When these two wavelengths are nearly the same, a small correction to f must be applied in precise work. An example is given in Sec. 13–4. Ordinarily we neglect this effect, called *anomalous dispersion*.

The scattering just discussed, whose amplitude is expressed in terms of the atomic scattering factor, is coherent, or unmodified, scattering, which is the only kind capable of being diffracted. On the other hand, incoherent, or Compton modified, scattering is occurring at the same time. Since the latter is due to collisions of quanta with loosely bound electrons, its intensity relative to that of the

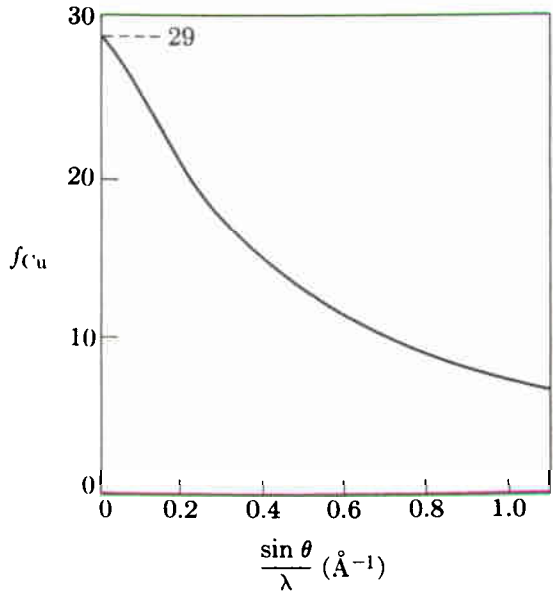

Fig. 4–6 The atomic scattering factor of copper.

unmodified radiation increases as the proportion of loosely bound electrons increases. The intensity of Compton modified radiation thus increases as the atomic number Z decreases. It is for this reason that it is difficult to obtain good diffraction photographs of organic materials, which contain light elements such as carbon, oxygen, and hydrogen, since the strong Compton modified scattering from these substances darkens the background of the photograph and makes it difficult to see the diffraction lines formed by the unmodified radiation. It is also found that the intensity of the modified radiation increases as the quantity $(\sin \theta)/\lambda$ increases. The intensities of modified scattering and of unmodified scattering therefore vary in opposite ways with Z and with $(\sin \theta)/\lambda$.

To summarize, when a monochromatic beam of x-rays strikes an atom, two scattering processes occur. Tightly bound electrons are set into oscillation and radiate x-rays of the same wavelength as that of the incident beam. More loosely bound electrons scatter part of the incident beam and slightly increase its wavelength in the process, the exact amount of increase depending on the scattering angle. The former is called coherent or unmodified scattering and the latter incoherent or modified; both kinds occur simultaneously and in all directions. If the atom is a part of a large group of atoms arranged in space in a regular periodic fashion as in a crystal, then another phenomenon occurs. The coherently scattered radiation from all the atoms undergoes reinforcement in certain directions and cancellation in other directions, thus producing diffracted beams. Diffraction is, essentially, reinforced coherent scattering.

We are now in a position to summarize, from the preceding sections and from Chap. 1, the chief effects associated with the passage of x-rays through matter. This is done schematically in Fig. 4–7. The incident x-rays are assumed to be of high enough energy, i.e., of short enough wavelength, to cause the emission of photoelectrons and characteristic fluorescent radiation. The Compton recoil electrons shown in the diagram are the loosely bound electrons knocked out of

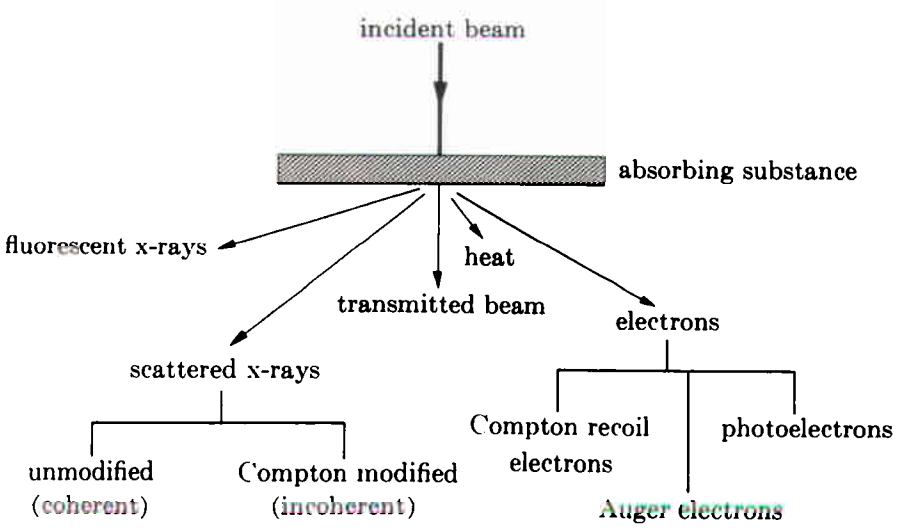

Fig. 4–7 Effects produced by the passage of x-rays through matter, after Henry, Lipson, and Wooster [G.8].

the atom by x-ray quanta, the interaction giving rise to Compton modified radiation. Auger electrons are those ejected from an atom by characteristic x-rays produced within the atom.

4–4 SCATTERING BY A UNIT CELL

To arrive at an expression for the intensity of a diffracted beam, we must now restrict ourselves to a consideration of the coherent scattering, not from an isolated atom but from all the atoms making up the crystal. The mere fact that the atoms are arranged in a periodic fashion in space means that the scattered radiation is now severely limited to certain definite directions and is now referred to as a set of diffracted beams. The directions of these beams are fixed by the Bragg law, which is, in a sense, a negative law. If the Bragg law is not satisfied, no diffracted beam can occur; however, the Bragg law may be satisfied for a certain set of atomic planes and yet no diffraction may occur, as in the example given at the beginning of this chapter, because of a particular arrangement of atoms within the unit cell [Fig. 4–2(b)].

Assuming that the Bragg law is satisfied, we wish to find the intensity of the beam diffracted by a crystal as a function of atom position. Since the crystal is merely a repetition of the fundamental unit cell, it is enough to consider the way in which the arrangement of atoms within a single unit cell affects the diffracted intensity.

Qualitatively, the effect is similar to the scattering from an atom, discussed in the previous section. There we found that phase differences occur in the waves scattered by the individual electrons, for any direction of scattering except the extreme forward direction. Similarly, the waves scattered by the individual atoms of a unit cell are not necessarily in phase except in the forward direction, and we must now determine how the phase difference depends on the arrangement of the atoms.

This problem is most simply approached by finding the phase difference between waves scattered by an atom at the origin and another atom whose position is variable in the x direction only. For convenience, consider an orthogonal unit cell, a section of which is shown in Fig. 4–8. Take atom A as the origin and let diffraction occur from the (h00) planes shown as heavy lines in the drawing. This means that the Bragg law is satisfied for this reflection and that $\delta_{2'1'}$, the path difference between ray **2′** and ray **1′**, is given by

$$\delta_{2'1'} = MCN = 2d_{h00} \sin \theta = \lambda.$$

From the definition of Miller indices,

$$d_{h00} = AC = \frac{a}{h}.$$

How is this reflection affected by x-rays scattered in the same direction by atom B, located at a distance x from A? Note that only this direction need be considered since only in this direction is the Bragg law satisfied for the h00 reflection. Clearly, the path difference between ray **3′** and ray **1′**, $\delta_{3'1'}$, will be less

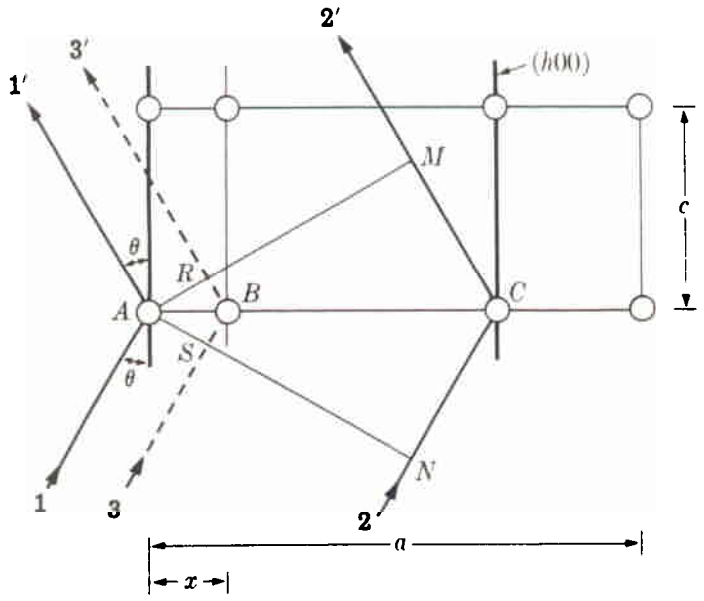

Fig. 4–8 The effect of atom position on the phase difference between diffracted rays.

than λ; by simple proportion it is found to be

$$\delta_{3'1'} = RBS = \frac{AB}{AC}(\lambda) = \frac{x}{a/h}(\lambda).$$

Phase differences may be expressed in angular measure as well as in wavelength: two rays, differing in path length by one whole wavelength, are said to differ in phase by 360°, or 2π radians. If the path difference is δ, then the phase difference ϕ in radians is given by

$$\phi = \frac{\delta}{\lambda}(2\pi).$$

The use of angular measure is convenient because it makes the expression of phase differences independent of wavelength, whereas the use of a path difference to describe a phase difference is meaningless unless the wavelength is specified.

The phase difference, then, between the wave scattered by atom B and that scattered by atom A at the origin is given by

$$\phi_{3'1'} = \frac{\delta_{3'1'}}{\lambda}(2\pi) = \frac{2\pi hx}{a}.$$

If the position of atom B is specified by its fractional coordinate $u = x/a$, then the phase difference becomes

$$\phi_{3'1'} = 2\pi hu.$$

This reasoning may be extended to three dimensions, as in Fig. 4–9, in which atom B has actual coordinates $x\ y\ z$ or fractional coordinates $\frac{x}{a}\ \frac{y}{b}\ \frac{z}{c}$ equal to $u\ v\ w$, respectively. We then arrive at the following important relation for the

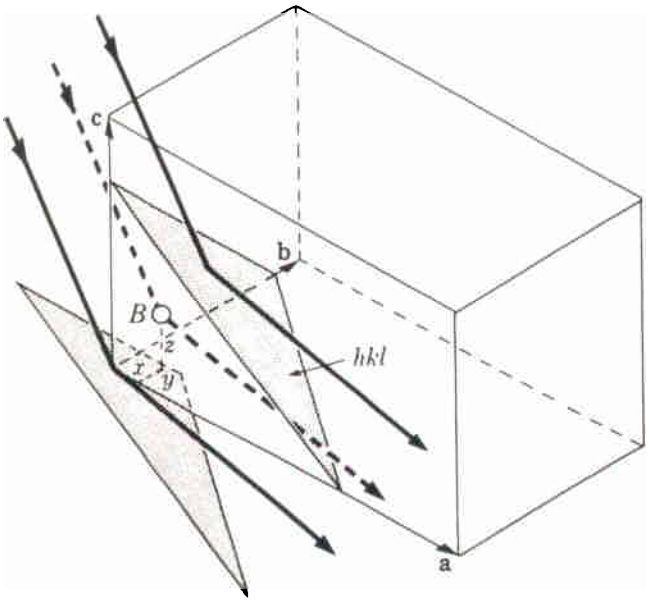

Fig. 4–9 The three-dimensional analogue of Fig. 4–8.

phase difference between the wave scattered by atom B and that scattered by atom A at the origin, for the hkl reflection:

$$\phi = 2\pi(hu + kv + lw). \tag{4–4}$$

This relation is general and applicable to a unit cell of any shape.

These two waves may differ, not only in phase, but also in amplitude if atom B and the atom at the origin are of different kinds. In that case, the amplitudes of these waves are given, relative to the amplitude of the wave scattered by a single electron, by the appropriate values of f, the atomic scattering factor.

We now see that the problem of scattering from a unit cell resolves itself into one of adding waves of different phase and amplitude in order to find the resultant wave. Waves scattered by all the atoms of the unit cell, including the one at the origin, must be added. The most convenient way of carrying out this summation is by expressing each wave as a complex exponential function.

The two waves shown as full lines in Fig. 4–10 represent the variations in electric field intensity E with time t of two rays on any given wave front in a diffracted x-ray beam. Their equations may be written

$$\mathbf{E}_1 = A_1 \sin(2\pi\nu t - \phi_1), \tag{4–5}$$

$$\mathbf{E}_2 = A_2 \sin(2\pi\nu t - \phi_2). \tag{4–6}$$

These waves are of the same frequency ν and therefore of the same wavelength λ, but differ in amplitude A and in phase ϕ. The dotted curve shows their sum $\mathbf{E}_3$, which is also a sine wave, but of different amplitude and phase.

Waves differing in amplitude and phase may also be added by representing them as vectors. In Fig. 4–11, each component wave is represented by a vector whose length is equal to the amplitude of the wave and which is inclined to the x-axis at an angle equal to the phase angle. The amplitude and phase of the

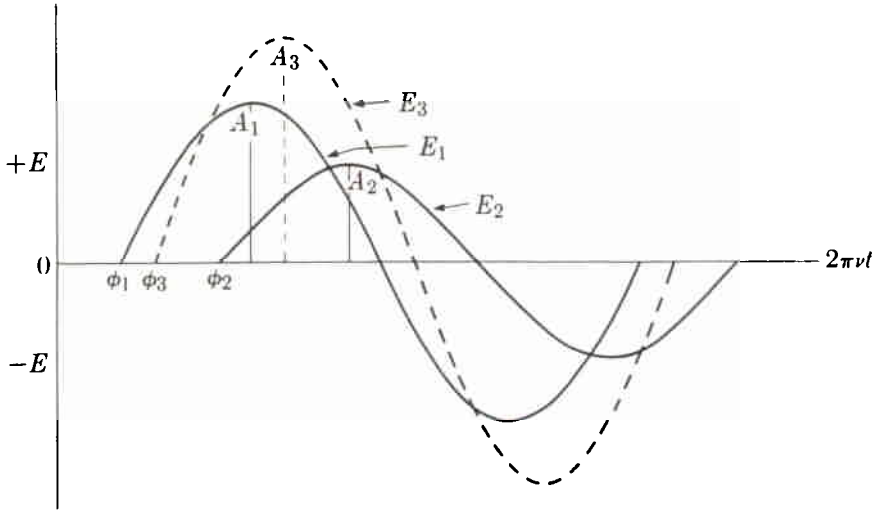

Fig. 4–10 The addition of sine waves of different phase and amplitude.

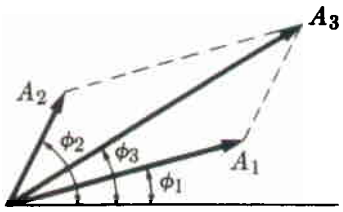

Fig. 4–11 Vector addition of waves.

resultant wave are then found simply by adding the vectors by the parallelogram law.

This geometrical construction may be avoided by use of the following analytical treatment, in which complex numbers are used to represent the vectors. A complex number is the sum of a real and an imaginary number, such as $(a + bi)$, where a and b are real and $i = \sqrt{-1}$ is imaginary. Such numbers may be plotted in the "complex plane," in which real numbers are plotted as abscissae and imaginary numbers as ordinates. Any point in this plane, or the vector drawn from the origin to this point, then represents a particular complex number $(a + bi)$.

To find an analytical expression for a vector representing a wave, we draw the wave vector in the complex plane as in Fig. 4–12. Here again the amplitude and phase of the wave are given by A, the length of the vector, and ϕ, the angle between the vector and the axis of real numbers. The analytical expression for the wave is now the complex number $(A \cos \phi + iA \sin \phi)$, since these two terms are the horizontal and vertical components OM and ON of the vector. Note that multiplication of a vector by i rotates it counterclockwise by 90°; thus multiplication by i converts the horizontal vector 2 into the vertical vector $2i$. Multiplication twice by i, that is, by $i^2 = -1$, rotates a vector through 180° or reverses its sense; thus multiplication twice by i converts the horizontal vector 2 into the horizontal vector -2 pointing in the opposite direction.

If we write down the power-series expansions of e^{ix}, $\cos x$, and $\sin x$ and

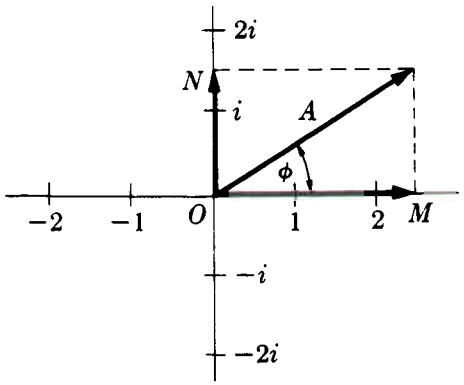

Fig. 4–12 A wave vector in the complex plane.

compare them, we find that

$$e^{ix} = \cos x + i \sin x \tag{4–7}$$

or

$$Ae^{i\phi} = A \cos \phi + Ai \sin \phi. \tag{4–8}$$

Thus the wave vector may be expressed analytically by either side of Eq. (4–8). The expression on the left is called a complex exponential function.

Since the intensity of a wave is proportional to the square of its amplitude, we now need an expression for A^2, the square of the absolute value of the wave vector. When a wave is expressed in complex form, this quantity is obtained by multiplying the complex expression for the wave by its complex conjugate, which is obtained simply by replacing i by $-i$. Thus, the complex conjugate of $Ae^{i\phi}$ is $Ae^{-i\phi}$. We have

$$|Ae^{i\phi}|^2 = Ae^{i\phi}Ae^{-i\phi} = A^2, \tag{4–9}$$

which is the quantity desired. Or, using the other form given by Eq. (4–8), we have

$$A(\cos \phi + i \sin \phi)A(\cos \phi - i \sin \phi) = A^2(\cos^2 \phi + \sin^2 \phi) = A^2.$$

We return now to the problem of adding the scattered waves from each of the atoms in the unit cell. The amplitude of each wave is given by the appropriate value of f for the scattering atom considered and the value of $(\sin \theta)/\lambda$ involved in the reflection. The phase of each wave is given by Eq. (4–4) in terms of the *hkl* reflection considered and the *uvw* coordinates of the atom. Using our previous relations, we can then express any scattered wave in the complex exponential form

$$Ae^{i\phi} = fe^{2\pi i(hu+kv+lw)}. \tag{4–10}$$

The resultant wave scattered by all the atoms of the unit cell is called the *structure factor*, because it describes how the atom arrangement, given by *uvw* for each atom, affects the scattered beam. The structure factor, designated by the symbol F, is obtained by simply adding together all the waves scattered by the individual atoms. If a unit cell contains atoms 1, 2, 3, . . . , N, with fractional coordinates $u_1\ v_1\ w_1, u_2\ v_2\ w_2, u_3\ v_3\ w_3, \ldots$ and atomic scattering factors $f_1, f_2, f_3, \ldots$, then the structure factor for the *hkl* reflection is given by

$$F = f_1e^{2\pi i(hu_1+kv_1+lw_1)} + f_2e^{2\pi i(hu_2+kv_2+lw_2)} + f_3e^{2\pi i(hu_3+kv_3+lw_3)} + \cdots.$$

This equation may be written more compactly as

$$F_{hkl} = \sum_{1}^{N} f_n e^{2\pi i(hu_n + kv_n + lw_n)}, \tag{4–11}$$

where the summation extends over all the N atoms of the unit cell.

F is, in general, a complex number, and it expresses both the amplitude and phase of the resultant wave. Its absolute value $|F|$ gives the amplitude of the resultant wave in terms of the amplitude of the wave scattered by a single electron. Like the atomic scattering factor f, $|F|$ is defined as a ratio of amplitudes:

$$|F| = \frac{\text{amplitude of the wave scattered by all the atoms of a unit cell}}{\text{amplitude of the wave scattered by one electron}}.$$

The intensity of the beam diffracted by all the atoms of the unit cell in a direction predicted by the Bragg law is proportional simply to $|F|^2$, the square of the amplitude of the resultant beam, and $|F|^2$ is obtained by multiplying the expression given for F in Eq. (4–11) by its complex conjugate. Equation (4–11) is therefore a very important relation in x-ray crystallography, since it permits a calculation of the intensity of any *hkl* reflection from a knowledge of the atomic positions.

We have found the resultant scattered wave by adding together waves, differing in phase, scattered by individual atoms in the unit cell. Note that the phase difference between rays scattered by any two atoms, such as A and B in Fig. 4–8, is *constant* for every unit cell. There is no question here of these rays becoming increasingly out of phase as we go deeper in the crystal as there was when we considered diffraction at angles not exactly equal to the Bragg angle θ_B. In the direction predicted by the Bragg law, the rays scattered by all the atoms A in the crystal are exactly in phase and so are the rays scattered by all the atoms B, but between these two sets of rays there is a definite phase difference which depends on the relative positions of atoms A and B in the unit cell and which is given by Eq. (4–4).

Although it is more unwieldy, the following trigonometric equation may be used instead of Eq. (4–11):

$$F = \sum_{1}^{N} f_n[\cos 2\pi(hu_n + kv_n + lw_n) + i \sin 2\pi(hu_n + kv_n + lw_n)].$$

One such term must be written down for each atom in the unit cell. In general, the summation will be a complex number of the form

$$F = a + ib,$$

where

$$a = \sum_1^N f_n \cos 2\pi(hu_n + kv_n + lw_n),$$

$$b = \sum_1^N f_n \sin 2\pi(hu_n + kv_n + lw_n),$$

$$|F|^2 = (a + ib)(a - ib) = a^2 + b^2.$$

Substitution for a and b gives the final form of the equation:

$$|F|^2 = [f_1 \cos 2\pi(hu_1 + kv_1 + lw_1) + f_2 \cos 2\pi(hu_2 + kv_2 + lw_2) + \cdots]^2 + [f_1 \sin 2\pi(hu_1 + kv_1 + lw_1) + f_2 \sin 2\pi(hu_2 + kv_2 + lw_2) + \cdots]^2.$$

Equation (4–11) is much easier to manipulate, compared to this trigonometric form, particularly if the structure is at all complicated, since the exponential form is more compact.

4–5 SOME USEFUL RELATIONS

In calculating structure factors by complex exponential functions, many particular relations occur often enough to be worthwhile stating here. They may be verified by means of Eq. (4–7).

a) $e^{\pi i} = e^{3\pi i} = e^{5\pi i} = -1,$

b) $e^{2\pi i} = e^{4\pi i} = e^{6\pi i} = +1,$

c) in general, $e^{n\pi i} = (-1)^n,$ where n is any integer,

d) $e^{n\pi i} = e^{-n\pi i},$ where n is any integer,

e) $e^{ix} + e^{-ix} = 2 \cos x.$

4–6 STRUCTURE-FACTOR CALCULATIONS

Facility in the use of Eq. (4–11) can be gained only by working out some actual examples, and we shall consider a few such problems here and again in Chap. 10.

a) The simplest case is that of a unit cell containing only one atom at the origin, i.e., having fractional coordinates 0 0 0. Its structure factor is

$$F = fe^{2\pi i(0)} = f$$

and

$$F^2 = f^2.$$

F^2 is thus independent of h, k, and l and is the same for all reflections.

b) Consider now the base-centered cell discussed at the beginning of this chapter and shown in Fig. 4–1(a). It has two atoms of the same kind per unit cell located at 0 0 0 and $\frac{1}{2}\ \frac{1}{2}\ 0$.

$$F = fe^{2\pi i(0)} + fe^{2\pi i(h/2+k/2)}$$

$$= f[1 + e^{\pi i(h+k)}].$$

This expression may be evaluated without multiplication by the complex conjugate,

since $(h + k)$ is always integral, and the expression for F is thus real and not complex. If h and k are both even or both odd, i.e., "unmixed," then their sum is always even and $e^{\pi i(h+k)}$ has the value 1. Therefore

$$F = 2f \qquad \text{for } h \text{ and } k \text{ unmixed;}$$
$$F^2 = 4f^2.$$

On the other hand, if h and k are one even and one odd, i.e., "mixed," then their sum is odd and $e^{\pi i(h+k)}$ has the value -1. Therefore

$$F = 0 \qquad \text{for } h \text{ and } k \text{ mixed;}$$
$$F^2 = 0.$$

Note that, in either case, the value of the l index has no effect on the structure factor. For example, the reflections 111, 112, 113, and 021, 022, 023 all have the same value of F, namely $2f$. Similarly, the reflections 011, 012, 013, and 101, 102, 103 all have a zero structure factor.

c) The structure factor of the body-centered cell shown in Fig. 4–1(b) may also be calculated. This cell has two atoms of the same kind located at 0 0 0 and $\frac{1}{2}\,\frac{1}{2}\,\frac{1}{2}$.

$$F = fe^{2\pi i(0)} + fe^{2\pi i(h/2+k/2+l/2)}$$
$$= f[1 + e^{\pi i(h+k+l)}].$$
$$F = 2f \qquad \text{when } (h + k + l) \text{ is even;}$$
$$F^2 = 4f^2.$$
$$F = 0 \qquad \text{when } (h + k + l) \text{ is odd;}$$
$$F^2 = 0.$$

We had previously concluded from geometrical considerations that the base-centered cell would produce a 001 reflection but that the body-centered cell would not. This result is in agreement with the structure-factor equations for these two cells. A detailed examination of the geometry of all possible reflections, however, would be a very laborious process compared to the straightforward calculation of the structure factor, a calculation that yields a set of rules governing the value of F^2 for all possible values of plane indices.

d) A face-centered cubic cell, such as that shown in Fig. 2–14, may now be considered. Assume it to contain four atoms of the same kind, located at 0 0 0, $\frac{1}{2}\,\frac{1}{2}$ 0, $\frac{1}{2}$ 0 $\frac{1}{2}$, and 0 $\frac{1}{2}\,\frac{1}{2}$.

$$F = fe^{2\pi i(0)} + fe^{2\pi i(h/2+k/2)} + fe^{2\pi i(h/2+l/2)} + fe^{2\pi i(k/2+l/2)}$$
$$= f[1 + e^{\pi i(h+k)} + e^{\pi i(h+l)} + e^{\pi i(k+l)}].$$

If h, k, and l are unmixed, then all three sums $(h + k)$, $(h + l)$, and $(k + l)$ are even integers, and each term in the above equation has the value 1.

$$F = 4f \qquad \text{for unmixed indices;}$$
$$F^2 = 16f^2.$$

If h, k, and l are mixed, then the sum of the three exponentials is -1, whether two of the indices are odd and one even, or two even and one odd. Suppose, for example, that h and l are even and k is odd, e.g., 012. Then $F = f(1 - 1 + 1 - 1) = 0$, and no reflection occurs.

$$F = 0 \qquad \text{for mixed indices;}$$
$$F^2 = 0$$

Thus, reflections will occur for such planes as (111), (200), and (220) but not for the planes (100), (210), (112), etc.

The reader may have noticed in the previous examples that some of the information given was not used in the calculations. In (a), for example, the cell was said to contain only one atom, but the shape of the cell was not specified; in (b) and (c), the cells were described as orthorhombic and in (d) as cubic, but this information did not enter into the structure-factor calculations. This illustrates the important point that *the structure factor is independent of the shape and size of the unit cell.* For example, *any* body-centered cell will have missing reflections for those planes which have $(h + k + l)$ equal to an odd number, whether the cell is cubic, tetragonal, or orthorhombic. The rules we have derived in the above examples are therefore of wider applicability than would at first appear and demonstrate the close connection between the Bravais lattice of a substance and its diffraction pattern. They are summarized in Table 4–1. These rules are subject to

Table 4–1

Bravais lattice	Reflections possibly present	Reflections necessarily absent
Simple	all	none
Base-centered	h and k unmixed*	h and k mixed*
Body-centered	$(h + k + l)$ even	$(h + k + l)$ odd
Face-centered	h, k, and l unmixed	h, k, and l mixed

* These relations apply to a cell centered on the C face. If reflections are present only when h and l are unmixed, or when k and l are unmixed, then the cell is centered on the B or A face, respectively.

some qualification, since some cells may contain more atoms than the ones given in examples (a) through (d), and these atoms may be in such positions that reflections normally present are now missing. For example, diamond has a face-centered cubic lattice, but it contains eight carbon atoms per unit cell. All the reflections present have unmixed indices, but reflections such as 200, 222, 420, etc., are missing. The fact that the only reflections *present* have unmixed indices proves that the lattice is face-centered, while the extra missing reflections are a clue to the actual atom arrangement in this crystal.

e) This point may be further illustrated by the structure of NaCl (Fig. 2–18). This crystal has a cubic lattice with 4 Na and 4 Cl atoms per unit cell, located as follows:

Na	0 0 0	$\frac{1}{2}\frac{1}{2}0$	$\frac{1}{2}0\frac{1}{2}$	$0\frac{1}{2}\frac{1}{2}$
Cl	$\frac{1}{2}\frac{1}{2}\frac{1}{2}$	$00\frac{1}{2}$	$0\frac{1}{2}0$	$\frac{1}{2}00$

In this case, the proper atomic scattering factors for each atom* must be inserted in the structure-factor equation, which will have eight terms:

$$F = f_{Na}e^{2\pi i(0)} + f_{Na}e^{2\pi i(h/2+k/2)} + f_{Na}e^{2\pi i(h/2+l/2)} + f_{Na}e^{2\pi i(k/2+l/2)} + f_{Cl}e^{2\pi i(h/2+k/2+l/2)} + f_{Cl}e^{2\pi i(l/2)} + f_{Cl}e^{2\pi i(k/2)} + f_{Cl}e^{2\pi i(h/2)},$$

$$F = f_{Na}[1 + e^{\pi i(h+k)} + e^{\pi i(h+l)} + e^{\pi i(k+l)}] + f_{Cl}[e^{\pi i(h+k+l)} + e^{\pi il} + e^{\pi ik} + e^{\pi ih}].$$

As discussed in Sec. 2–7, the sodium-atom positions are related by the face-centering translations and so are the chlorine-atom positions. *Whenever a lattice contains common translations, the corresponding terms in the structure-factor equation can always be factored out*, leading to considerable simplification. In this case we proceed as follows:

$$F = f_{Na}[1 + e^{\pi i(h+k)} + e^{\pi i(h+l)} + e^{\pi i(k+l)}] + f_{Cl}e^{\pi i(h+k+l)}[1 + e^{\pi i(-h-k)} + e^{\pi i(-h-l)} + e^{\pi i(-k-l)}].$$

The signs of the exponents in the second bracket may be changed, by relation (d) of Sec. 4–5. Therefore

$$F = [1 + e^{\pi i(h+k)} + e^{\pi i(h+l)} + e^{\pi i(k+l)}][f_{Na} + f_{Cl}e^{\pi i(h+k+l)}].$$

Here the terms corresponding to the face-centering translations appear in the first factor; the second factor contains the terms that describe the "basis" of the unit cell, namely, the Na atom at 0 0 0 and the Cl atom at $\frac{1}{2}\ \frac{1}{2}\ \frac{1}{2}$. The terms in the first bracket, describing the face-centering translations, have already appeared in example (d), and they were found to have a total value of zero for mixed indices and 4 for unmixed indices. This shows at once that NaCl has a face-centered lattice and that

$$F = 0 \qquad \text{for mixed indices;}$$
$$F^2 = 0.$$

For unmixed indices,

$$F = 4[f_{Na} + f_{Cl}e^{\pi i(h+k+l)}].$$
$$F = 4(f_{Na} + f_{Cl}) \qquad \text{if } (h + k + l) \text{ is even;}$$
$$F^2 = 16(f_{Na} + f_{Cl})^2.$$
$$F = 4(f_{Na} - f_{Cl}) \qquad \text{if } (h + k + l) \text{ is odd;}$$
$$F^2 = 16(f_{Na} - f_{Cl})^2.$$

In this case, there are more than four atoms per unit cell, but the lattice is still face-centered. The introduction of additional atoms has not eliminated any reflections present in the case of the four-atom cell, but it has decreased some in intensity. For example, the 111 reflection now involves the difference, rather than the sum, of the scattering powers of the two atoms.

* Strictly, and if the calculation of F is to be made to the highest accuracy, scattering factors f for the ions Na^+ and Cl^- must be used, rather than the f values for the neutral atoms Na and Cl, because NaCl is ionized.

The student should carefully note that a lot of algebra can be eliminated, whenever a lattice is known to be centered in any way, by factoring common translations out of the structure-factor equation and inserting immediately the known values of the terms representing these translations. This shortcut procedure is illustrated for NaCl:

1. Write down the atom positions in abbreviated form:

4 Na at 0 0 0 + face-centering translations,

4 Cl at $\frac{1}{2}\ \frac{1}{2}\ \frac{1}{2}$ + face-centering translations.

2. Write down the equation for F as a product of two factors. The first is the value of the terms representing the common translations; the second has terms corresponding to the "basis" atoms of the cell. The equation is

$$F = \begin{bmatrix}4\\0\end{bmatrix} [f_{\mathrm{Na}} + f_{\mathrm{Cl}} e^{\pi i(h+k+l)}] \qquad \begin{matrix}\text{unmixed indices}\\ \text{mixed indices.}\end{matrix}$$

3. Simplify further, as necessary. In all structure-factor calculations the aim is to obtain a set of *general* equations that will give the value of F for *any* value of hkl.

This shortcut procedure is illustrated again, for the ZnS structure, in Sec. 4–13.

f) One other example of structure factor calculation will be given here. The close-packed hexagonal cell shown in Fig. 2–15 has two atoms of the same kind located at 0 0 0 and $\frac{1}{3}\ \frac{2}{3}\ \frac{1}{2}$.

$$\begin{aligned} F &= fe^{2\pi i(0)} + fe^{2\pi i(h/3 + 2k/3 + l/2)} \\ &= f[1 + e^{2\pi i[(h+2k)/3 + l/2]}]. \end{aligned}$$

For convenience, put $[(h + 2k)/3 + l/2] = g$.

$$F = f(1 + e^{2\pi i g}).$$

Since g may have fractional values, such as $\frac{1}{3}$, $\frac{2}{3}$, $\frac{5}{6}$, etc., this expression is still complex. Multiplication by the complex conjugate, however, will give the square of the absolute value of the resultant wave amplitude F.

$$\begin{aligned} |F|^2 &= f^2(1 + e^{2\pi i g})(1 + e^{-2\pi i g}) \\ &= f^2(2 + e^{2\pi i g} + e^{-2\pi i g}). \end{aligned}$$

By relation (e) of Sec. 4–5, this becomes

$$\begin{aligned} |F|^2 &= f^2(2 + 2\cos 2\pi g) \\ &= f^2[2 + 2(2\cos^2 \pi g - 1)] \\ &= f^2(4\cos^2 \pi g) \\ &= 4f^2 \cos^2 \pi \left(\frac{h + 2k}{3} + \frac{l}{2}\right) \\ &= 0 \qquad \text{when } (h + 2k) \text{ is a multiple of 3 and } l \text{ is odd.} \end{aligned}$$

It is by these missing reflections, such as $11 \cdot 1$, $11 \cdot 3$, $22 \cdot 1$, $22 \cdot 3$, that a hexagonal structure is recognized as being close-packed. Not all the reflections present have the same structure factor. For example, if $(h + 2k)$ is a multiple of 3 and l is even, then

$$\left(\frac{h + 2k}{3} + \frac{l}{2}\right) = n, \qquad \text{where } n \text{ is an integer;}$$

$$\cos \pi n = \pm 1,$$

$$\cos^2 \pi n = 1,$$

$$|F|^2 = 4f^2.$$

When all possible values of h, k, and l are considered, the results may be summarized as follows, where m is an integer:

$h + 2k$	l	$\lvert F\rvert^2$
$3m$	odd	0
$3m$	even	$4f^2$
$3m \pm 1$	odd	$3f^2$
$3m \pm 1$	even	f^2

4–7 APPLICATION TO POWDER METHOD

Any calculation of the intensity of a diffracted beam must always begin with the structure factor. The remainder of the calculation, however, varies with the particular diffraction method involved. For the Laue method, intensity calculations are so difficult that they are rarely made, since each diffracted beam has a different wavelength and blackens the film by a variable amount, depending on both the intensity and the film sensitivity for that particular wavelength. The factors governing diffracted intensity in the rotating-crystal and powder methods are somewhat similar, in that monochromatic radiation is used in each, but they differ in detail. The remainder of this chapter will be devoted to the powder method, since it is of most general utility in metallurgical work.

There are six factors affecting the relative intensity of the diffraction lines on a powder pattern:

1. polarization factor,
2. structure factor,
3. multiplicity factor,
4. Lorentz factor,
5. absorption factor,
6. temperature factor.

The first two of these have already been described, and the others will be discussed in the following sections.

4–8 MULTIPLICITY FACTOR

Consider the 100 reflection from a cubic lattice. In the powder specimen, some of the crystals will be so oriented that reflection can occur from their (100) planes. Other crystals of different orientation may be in such a position that reflection can occur from their (010) or (001) planes. Since all these planes have the same spacing, the beams diffracted by them all form part of the same cone. Now consider the 111 reflection. There are four sets of planes of the form {111} which have the same spacing but different orientation, namely, (111), (11$\bar{1}$), (1$\bar{1}\bar{1}$), and (1$\bar{1}$1), whereas there are only three sets of the form {100}. Therefore, the probability that {111} planes will be correctly oriented for reflection is $\frac{4}{3}$ the probability that {100} planes will be correctly oriented. It follows that the intensity of the 111 reflection will be $\frac{4}{3}$ that of the 100 reflection, other things being equal.

This relative proportion of planes contributing to the same reflection enters the intensity equation as the quantity p, the *multiplicity factor*, which may be defined as the number of different planes in a form having the same spacing. Parallel planes with different Miller indices, such as (100) and ($\bar{1}$00), are counted separately as different planes, yielding numbers which are double those given in the preceding paragraph. Thus the multiplicity factor for the {100} planes of a cubic crystal is 6 and for the {111} planes 8.

The value of p depends on the crystal system: in a tetragonal crystal, the (100) and (001) planes do not have the same spacing, so that the value of p for {100} planes is reduced to 4 and the value for {001} planes to 2. Values of the multiplicity factor as a function of hkl and crystal system are given in Appendix 13.

4–9 LORENTZ FACTOR

We must now consider certain trigonometrical factors which influence the intensity of the reflected beam. Suppose there is incident on a crystal [Fig. 4–13(a)] a narrow beam of parallel monochromatic rays, and let the crystal be rotated at a uniform angular velocity about an axis through O and normal to the drawing, so that a particular set of reflecting planes, assumed for convenience to be parallel to the crystal surface, passes through the angle θ_B, at which the Bragg law is exactly satisfied. As mentioned in Sec. 3–7, the intensity of reflection is greatest at the exact Bragg angle but still appreciable at angles deviating slightly from the Bragg angle, so that a curve of intensity vs. 2θ is of the form shown in Fig. 4–13(b). If all the diffracted beams sent out by the crystal as it rotates through the Bragg angle are received on a photographic film or in a counter, the total energy of the diffracted beam can be measured. This energy is called the *integrated intensity* of the reflection and is given by the area under the curve of Fig. 4–13(b). The integrated intensity is of much more interest than the maximum intensity, since the former is characteristic of the specimen while the latter is influenced by slight adjustments of the experimental apparatus. Moreover, in the visual comparison of the intensities of diffraction lines, it is the integrated intensity of the line rather than the maximum intensity which the eye evaluates.

The integrated intensity of a reflection depends on the particular value of θ_B

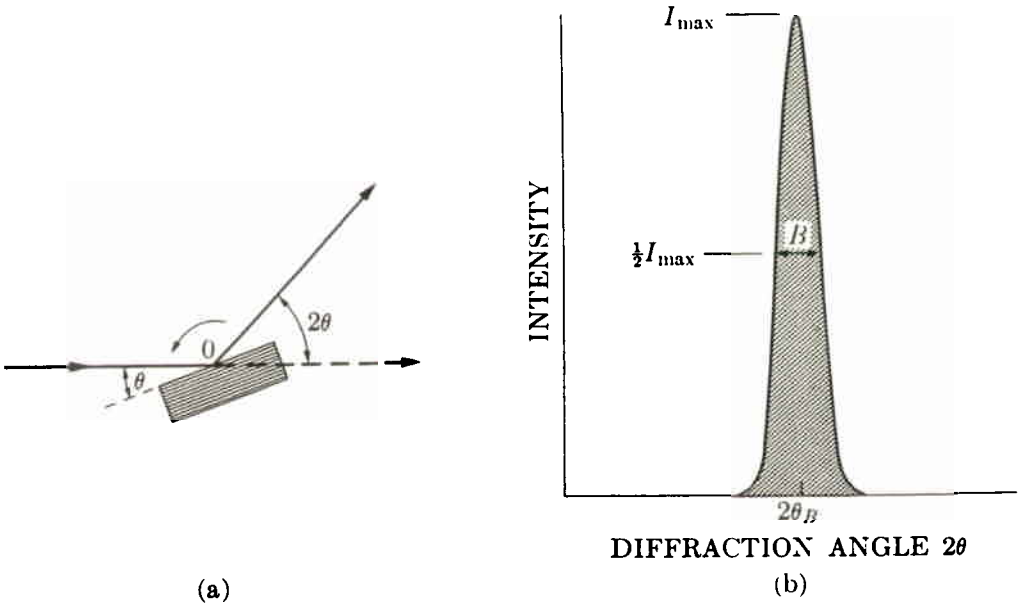

Fig. 4–13 Diffraction by a crystal rotated through the Bragg angle.

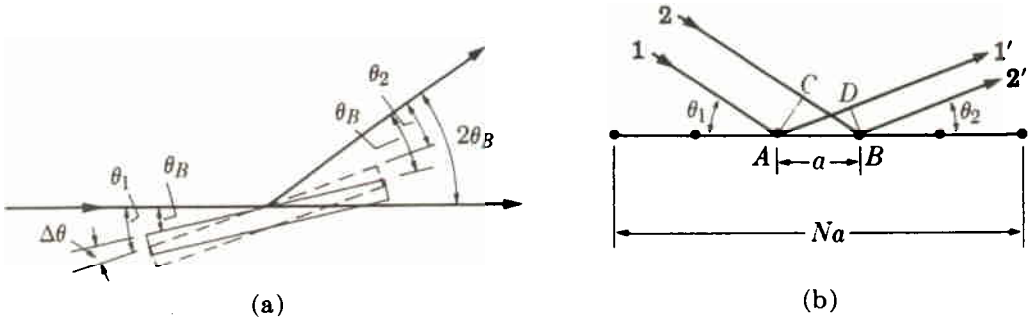

Fig. 4–14 Scattering in a fixed direction during crystal rotation.

involved, even though all other variables are held constant. We can find this dependence by considering, separately, two aspects of the diffraction curve: the maximum intensity and the breadth. When the reflecting planes make an angle θ_B with the incident beam, the Bragg law is exactly satisfied and the intensity diffracted in the direction $2\theta_B$ is a maximum. But some energy is still diffracted in this direction when the angle of incidence differs slightly from θ_B, and the total energy diffracted in the direction $2\theta_B$ as the crystal is rotated through the Bragg angle is given by the value of I_{max} of the curve of Fig. 4–13(b). The value of I_{max} therefore depends on the angular range of crystal rotation over which the energy diffracted in the direction $2\theta_B$ is appreciable. In Fig. 4–14(a), the dashed lines show the position of the crystal after rotation through a small angle $\Delta\theta$ from the Bragg position. The incident beam and the diffracted beam under consideration now make unequal angles with the reflecting planes, the former making an angle $\theta_1 = \theta_B + \Delta\theta$ and the latter an angle $\theta_2 = \theta_B - \Delta\theta$. The situation on an atomic scale is shown in Fig. 4–14(b). Here we need only consider a single plane of atoms, since the rays scattered by all other planes are in phase with the corresponding rays

scattered by the first plane. Let a equal the atom spacing in the plane and Na the total length* of the plane. The difference in path length for rays $\mathbf{1}'$ and $\mathbf{2}'$ scattered by adjacent atoms is given by

$$\begin{aligned}\delta_{1'2'} &= AD - CB \\ &= a\cos\theta_2 - a\cos\theta_1 \\ &= a[\cos(\theta_B - \Delta\theta) - \cos(\theta_B + \Delta\theta)].\end{aligned}$$

By expanding the cosine terms and setting $\sin\Delta\theta$ equal to $\Delta\theta$, since the latter is small, we find:

$$\delta_{1'2'} = 2a\,\Delta\theta\sin\theta_B,$$

and the path difference between the rays scattered by atoms at either end of the plane is simply N times this quantity. When the rays scattered by the two end atoms are one wavelength out of phase, the diffracted intensity will be zero. (The argument here is exactly analogous to that used in Sec. 3–7.) The condition for zero diffracted intensity is therefore

$$2Na\,\Delta\theta\sin\theta_B = \lambda,$$

or

$$\Delta\theta = \frac{\lambda}{2Na\sin\theta_B}.$$

This equation gives the maximum angular range of crystal rotation over which appreciable energy will be diffracted in the direction $2\theta_B$. Since I_{max} depends on this range, we can conclude that I_{max} is proportional to $1/\sin\theta_B$. Other things being equal, I_{max} is therefore large at low scattering angles and small in the back-reflection region.

The breadth of the diffraction curve varies in the opposite way, being larger at large values of $2\theta_B$, as was shown in Sec. 3–7, where the half-maximum breadth B was found to be proportional to $1/\cos\theta_B$. The integrated intensity of the reflection is given by the area under the diffraction curve and is therefore proportional to the product $I_{max}\,B$, which is in turn proportional to $(1/\sin\theta_B)(1/\cos\theta_B)$ or to $1/\sin 2\theta_B$. Thus, as a crystal is rotated through the Bragg angle, the integrated intensity of a reflection, which is the quantity of most experimental interest, turns out to be greater for large and small values of $2\theta_B$ than for intermediate values, other things being equal.

The preceding remarks apply just as well to the powder method as they do to the case of a rotating crystal, since the range of orientations available among the powder particles, some satisfying the Bragg law exactly, some not so exactly, are the equivalent of single-crystal rotation.

However, in the powder method, a second geometrical factor arises when we consider that the integrated intensity of a reflection at any particular Bragg angle depends on the number of crystals oriented at or near that angle. This number is

* If the crystal is larger than the incident beam, then Na is the irradiated length of the plane; if it is smaller, Na is the actual length of the plane.

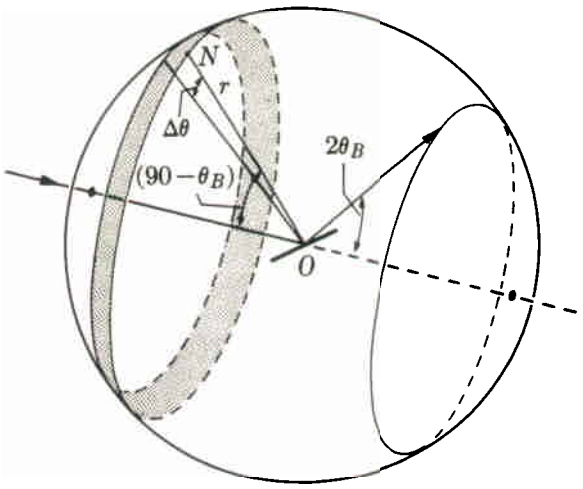

Fig. 4–15 The distribution of plane normals for a particular cone of reflected rays.

not constant even though the crystals are oriented completely at random. In Fig. 4–15 a reference sphere of radius r is drawn around the powder specimen located at O. For the particular hkl reflection shown, ON is the normal to this set of planes in one crystal of the powder. Suppose that the range of angles near the Bragg angle over which reflection is appreciable is $\Delta\theta$. Then, for this particular reflection, only those crystals will be in a reflecting position which have the ends of their plane normals lying in a band of width $r\,\Delta\theta$ on the surface of the sphere. Since the crystals are assumed to be oriented at random, the ends of their plane normals will be uniformly distributed over the surface of the sphere; the fraction favorably oriented for a reflection will be given by the ratio of the area of the strip to that of the whole sphere. If ΔN is the number of such crystals and N the total number, then

$$\frac{\Delta N}{N} = \frac{r\,\Delta\theta \cdot 2\pi r \sin(90^\circ - \theta_B)}{4\pi r^2} = \frac{\Delta\theta \cos\theta_B}{2}.$$

The number of crystals favorably oriented for reflection is thus proportional to $\cos\theta_B$ and is quite small for reflections in the backward direction.

In assessing relative intensities, we do not compare the total diffracted energy in one cone of rays with that in another but rather the integrated intensity per unit length of one diffraction line with that of another. For example, in the most common arrangement of specimen and film, the Debye–Scherrer method, shown in Fig. 4–16, the film obviously receives a greater proportion of a diffraction cone when the reflection is in the forward or backward direction than it does near $2\theta = 90^\circ$. Inclusion of this effect thus leads to a third geometrical factor affecting the intensity of a reflection. The length of any diffraction line being $2\pi R \sin 2\theta_B$, where R is the radius of the camera, the relative intensity per unit length of line is proportional to $1/\sin 2\theta_B$.

In intensity calculations, the three factors just discussed are combined into one and called the Lorentz factor. Dropping the subscript on the Bragg angle, we have:

$$\text{Lorentz factor} = \left(\frac{1}{\sin 2\theta}\right)(\cos\theta)\left(\frac{1}{\sin 2\theta}\right) = \frac{\cos\theta}{\sin^2 2\theta} = \frac{1}{4\sin^2\theta\cos\theta}.$$

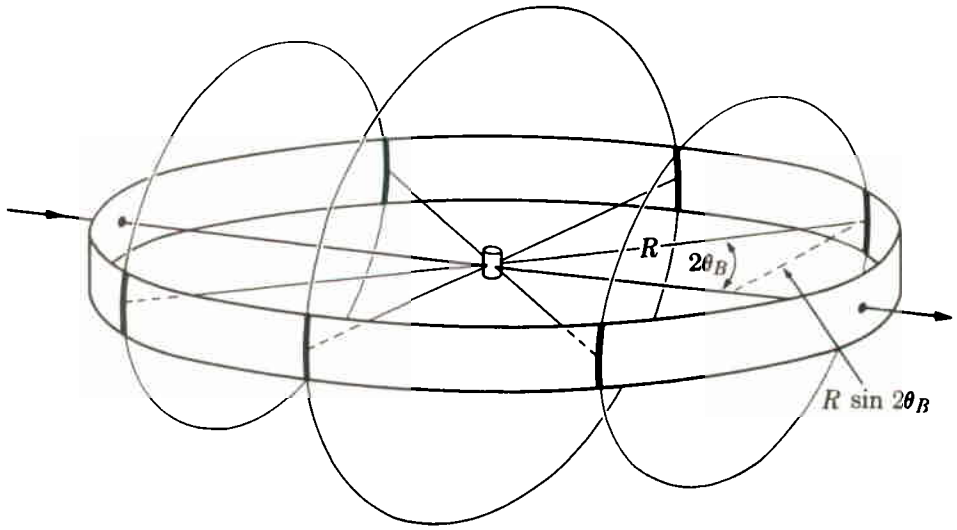

Fig. 4–16 Intersection of cones of diffracted rays with Debye-Scherrer film.

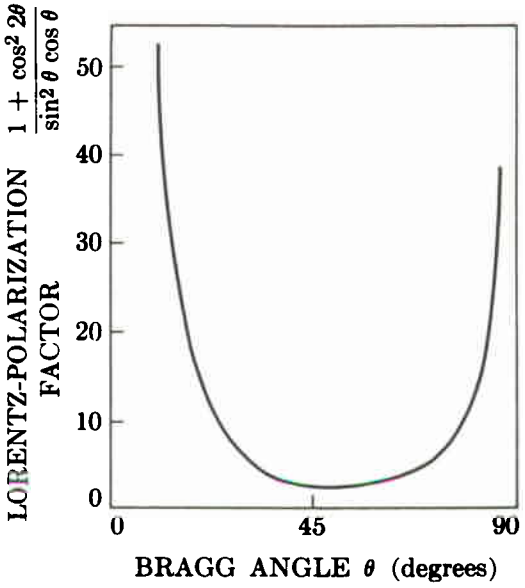

Fig. 4–17 Lorentz-polarization factor.

This in turn is combined with the polarization factor $\frac{1}{2}(1 + \cos^2 2\theta)$ of Sec. 4–2 to give the combined Lorentz-polarization factor which, with a constant factor of $\frac{1}{8}$ omitted, is given by

$$\text{Lorentz-polarization factor} = \frac{1 + \cos^2 2\theta}{\sin^2 \theta \cos \theta}.$$

Values of this factor are given in Appendix 14 and plotted in Fig. 4–17 as a function of θ. The overall effect of these geometrical factors is to decrease the intensity of reflections at intermediate angles compared to those in forward or backward directions.

4–10 ABSORPTION FACTOR

Still another factor affecting the intensities of the diffracted rays must be considered, and that is the absorption which takes place in the specimen itself. We allow for this effect in intensity calculations by introducing the *absorption factor A*, which is a number by which the calculated intensity is to be multiplied to allow for absorption. The calculation of A depends on the geometry of the diffraction method involved, and we will consider below the two most-used methods.

Debye–Scherrer Camera

The specimen in the Debye–Scherrer method has the form of a very thin cylinder of powder placed on the camera axis, and Fig. 4–18(a) shows the cross section of such a specimen. For the low-angle reflection shown, absorption of a particular ray in the incident beam occurs along a path such as AB; at B a small fraction of the incident energy is diffracted by a powder particle, and absorption of this diffracted beam occurs along the path BC. Similarly, for a high-angle reflection, absorption of both the incident and diffracted beams occurs along a path such as $(DE + EF)$. The net result is that the diffracted beam is of lower intensity than one would expect for a specimen of no absorption.

A calculation of this effect shows that the relative absorption increases as θ decreases, for any given cylindrical specimen. That this must be so can be seen from Fig. 4–18(b) which applies to a specimen (for example, tungsten) of very high absorption. The incident beam is very rapidly absorbed, and most of the diffracted beams originate in the thin surface layer on the left side of the specimen; backward-reflected beams then undergo very little absorption, but forward-reflected beams have to pass through the whole specimen and are greatly absorbed. Actually, the forward-reflected beams in this case come almost entirely from the top and bottom

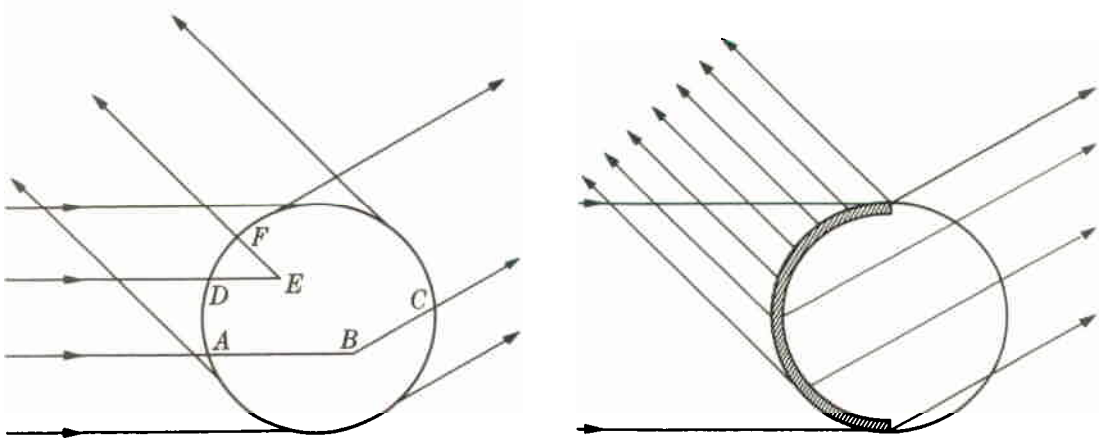

(a) (b)

Fig. 4–18 Absorption in Debye–Scherrer specimens: (a) general case, (b) highly absorbing specimen.

edges of the specimen.* This difference in absorption between high-θ and low-θ reflections decreases as the linear absorption coefficient decreases, but the absorption is always greater for the low-θ reflections. We therefore write the Debye–Scherrer absorption factor as $A(\theta)$ to emphasize the fact that it varies with θ. Qualitatively, we conclude that $A(\theta)$ for any specimen increases as 2θ increases.

Exact calculation of the absorption factor for a cylindrical specimen is often difficult, so it is fortunate that this effect can usually be neglected in the calculation of diffracted intensities, when the Debye–Scherrer method is used. Justification of this omission will be found in Sec. 4–11.

The calculation of $A(\theta)$ for a cylindrical specimen proceeds as follows. In Fig. 4–18(a) the path length $(AB + BC)$, for a given value of θ, is expressed as a function of the position x, y of the point B relative to coordinate axes fixed relative to the specimen. The absorption factor $A(\theta)$ is then given by the function $e^{-\mu(AB+BC)}$ integrated over the entire cross-sectional area of the specimen. This integration can only be performed numerically. The result is a table of values of $A(\theta)$ as a function of θ and of the product μr, where μ is the linear absorption coefficient of the specimen and r is its radius. The specimen is usually a powder compact, with an absorption coefficient given by

$$\mu_{\text{compact}} = \mu_{\text{solid}} \left(\frac{\rho_{\text{compact}}}{\rho_{\text{solid}}} \right) \tag{4–12}$$

where ρ is density.

Values of $A(\theta)$ have been calculated and tabulated by Bradley [4.1]. Tables of values can also be found in [G.11, Vol. 2, p. 295–299] and in [G.13, p. 663–666].

Diffractometer

A diffractometer specimen usually has the form of a flat plate making equal angles with the incident and diffracted beams as in Fig. 3–4, if one imagines a polycrystalline plate substituted for the single crystal indicated there. It is shown below that the absorption factor A is equal to $1/2\mu$, *independent of* θ. This independence of θ is due to the exact balancing of two opposing effects. When θ is small, the specimen area irradiated by an incident beam of fixed cross section is large, but the effective depth of x-ray penetration is small; when θ is large, the irradiated area is small, but the penetration depth is relatively large. The net effect is that the effective irradiated volume is constant and independent of θ. Absorption occurs in any case, however, and the larger the absorption coefficient of the specimen, the lower the intensity of the diffracted beams, other things being equal. The important fact to note is that absorption decreases the intensities of all diffracted beams by the same factor and therefore does not enter into the calculation of *relative* intensities.

* The powder patterns reproduced in Fig. 3–13 show this effect, at least on the original films. The lowest-angle line in each pattern is split in two, because the beam diffracted through the center of the specimen is so highly absorbed. It is important to keep the possibility of this phenomenon in mind when examining Debye–Scherrer photographs, or split low-angle lines may be incorrectly interpreted as separate diffraction lines from two different sets of planes.

The calculation of A proceeds as follows. The incident beam in the diffractometer is actually divergent (Sec. 7–2), but we will assume here that the beam is composed of parallel rays, because the divergence angle is very small (3° or less). We will calculate the effect of absorption in the specimen on the intensity of the diffracted beam, and, since this effect will come up again in later parts of this book, we will make our calculation quite general. In Fig. 4–19, the incident beam has intensity I_0 (ergs/cm^2/sec), is 1 cm square in cross section, and is incident on the powder plate at an angle γ. We consider the energy diffracted from this beam by a layer of the powder of length l and thickness dx, located at a depth x below the surface. Since the incident beam undergoes absorption by the specimen over the path length AB, the energy incident per second on the layer considered is $I_0 e^{-\mu(AB)}$ (ergs/sec), where μ is the linear absorption coefficient of the powder compact, given by Eq. (4–12). Let a be the volume fraction of the specimen containing particles having the correct orientation for reflection of the incident beam, and b the fraction of the incident energy which is diffracted by unit volume. Then the energy diffracted per second by the layer considered, which has a volume l dx, is given by $abll_0 e^{-\mu(AB)}$ dx. But this diffracted energy is also decreased by absorption, by a factor of $e^{-\mu(BC)}$, since the diffracted rays have a path length of BC in the specimen. The energy flux per second in the diffracted beam outside the specimen, i.e., the integrated intensity, is therefore given by

$$dI_D = abll_0 e^{-\mu(AB+BC)}\, dx \quad \text{(ergs/sec)}. \tag{4–13}$$

But

$$l = \frac{1}{\sin\gamma}, \qquad AB = \frac{x}{\sin\gamma}, \qquad BC = \frac{x}{\sin\beta}.$$

Therefore,

$$dI_D = \frac{I_0 ab}{\sin\gamma}\, e^{-\mu x(1/\sin\gamma + 1/\sin\beta)}\, dx. \tag{4–14}$$

(The reader might note that the analogous absorption effect in transmission, rather than reflection, is given later as Eq. (9–7.)

For the particular specimen arrangement used in the diffractometer, $\gamma = \beta = \theta$, and the above equation becomes

$$dI_D = \frac{I_0 ab}{\sin\theta}\, e^{-2\mu x/\sin\theta}\, dx. \tag{4–15}$$

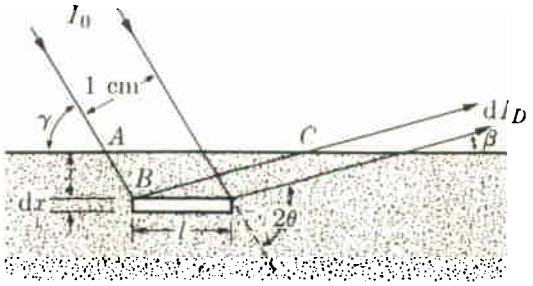

Fig. 4–19 Diffraction from a flat plate: incident and diffracted beams have a thickness of 1 cm in a direction normal to the plane of the drawing.

The total diffracted intensity is obtained by integrating over an infinitely thick specimen:

$$I_D = \int_{x=0}^{x=\infty} dI_D = \frac{I_0 ab}{2\mu}. \tag{4–16}$$

Here I_0, b, and μ are constant for all reflections (independent of θ) and we may also regard a as constant. Actually, a varies with θ, but this variation is already taken care of by the cos θ portion of the Lorentz factor (see Sec. 4–9) and need not concern us here. We conclude that the absorption factor $1/2\mu$ is independent of θ for a flat specimen making equal angles with the incident and diffracted beams, provided the specimen fills the incident beam at all angles and is effectively of infinite thickness.

The criterion adopted for "infinite thickness" depends on the sensitivity of our intensity measurements or on what we regard as negligible diffracted intensity. For example, we might arbitrarily but quite reasonably define infinite thickness as that thickness t which a specimen must have in order that the intensity diffracted by a thin layer on the back side be $\frac{1}{1000}$ of the intensity diffracted by a thin layer on the front side. Then, from Eq. (4–15) we have

$$\frac{dI_D \text{ (at } x = 0)}{dI_D \text{ (at } x = t)} = e^{2\mu t/\sin\theta} = 1000,$$

from which

$$t = \frac{3.45 \sin\theta}{\mu}.$$

This expression shows that "infinite thickness," for a metal specimen, is very small indeed. For example, suppose a specimen of nickel powder is being examined with Cu $K\alpha$ radiation at θ values approaching 90°. The density of the powder compact may be taken as about 0.6 the density of bulk nickel, which is 8.9 gm/cm^3, leading to a value of μ for the compact of 261 cm^{-1}. The value of t is therefore 1.32×10^{-2} cm, or about five thousandths of an inch.

4–11 TEMPERATURE FACTOR

So far we have considered a crystal as a collection of atoms located at fixed points in the lattice. Actually, the atoms undergo thermal vibration about their mean positions even at the absolute zero of temperature, and the amplitude of this vibration increases as the temperature increases. In aluminum at room temperature, the average displacement of an atom from its mean position is about 0.17 Å, which is by no means negligible, being about 6 percent of the distance of closest approach of the mean atom positions in this crystal.

Increased thermal vibration of the atoms, as the result of an increase in temperature, has three main effects:

1. The unit cell expands, causing changes in plane spacings d and therefore in the 2θ positions of the diffraction lines. If the positions of one or more lines are

measured as a function of temperature (Sections 6–5 and 7–2), the thermal expansion coefficient of the specimen can be determined by x-ray diffraction.

2. The intensities of the diffraction lines decrease.
3. The intensity of the background scattering between lines increases.

The second and third effects are described below. Here we are usually interested not in intensity changes with temperature, but in variations in intensity with 2θ at constant temperature (usually room temperature).

Thermal agitation decreases the intensity of a diffracted beam because it has the effect of smearing out the lattice planes; atoms can be regarded as lying no longer on mathematical planes but rather in platelike regions of ill-defined thickness. Thus the reinforcement of waves scattered at the Bragg angle by various parallel planes, the reinforcement which is called a diffracted beam, is not as perfect as it is for a crystal with fixed atoms. This reinforcement requires that the path difference, which is a function of the plane spacing d, between waves scattered by adjacent planes be an integral number of wavelengths. Now the thickness of the platelike "planes" in which the vibrating atoms lie is, on the average, $2u$, where u is the average displacement of an atom from its mean position. Under these conditions reinforcement is no longer perfect, and it becomes more imperfect as the ratio u/d increases, i.e., as the temperature increases, since that increases u, or as θ increases, since high-θ reflections involve planes of low d value. Thus the intensity of a diffracted beam decreases as the temperature is raised, and, for a constant temperature, thermal vibration causes a greater decrease in the reflected intensity at high angles than at low angles. In intensity calculations we allow for this effect by introducing the *temperature factor* e^{-2M}, which is a number by which the calculated intensity is to be multiplied to allow for thermal vibration of the atoms. Qualitatively, we conclude that e^{-2M} decreases as 2θ increases. A method of calculating e^{-2M} when it is needed is outlined later, and Fig. 4–20 shows the result of such a calculation for iron.

The temperature effect and the previously discussed absorption effect in cylindrical specimens depend on angle in opposite ways and, to a first approximation, cancel each other in the Debye-Scherrer method. In back reflection, for

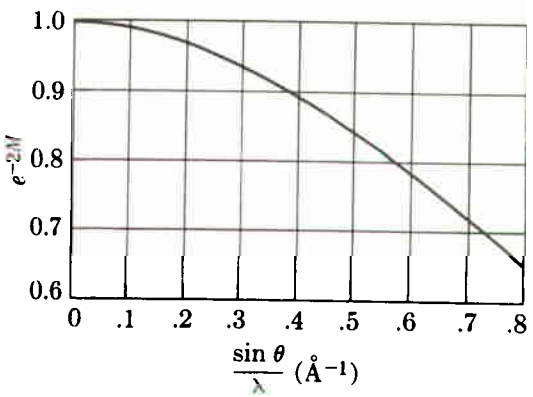

Fig. 4–20 Temperature factor e^{-2M} of iron at 20°C as a function of $(\sin\theta)/\lambda$.

example, the intensity of a diffracted beam is decreased very little by absorption but very greatly by thermal agitation, while in the forward direction the reverse is true. The two effects do not exactly cancel one another at all angles; however, if the comparison of line intensities is restricted to lines not differing too greatly in θ values, the absorption and temperature effects can be safely ignored in the Debye-Scherrer method. This is a fortunate circumstance, since both of these effects are rather difficult to calculate exactly.

Theoretically, thermal vibration of the atoms causes a very slight increase in the breadth B, measured at half-maximum intensity, of the diffraction lines. However, this expected effect has never been detected [4.2], and diffraction lines are observed to be sharp right up to the melting point, but their maximum intensity gradually decreases.

It is also worth noting that the mean amplitude of atomic vibration is not a function of the temperature alone but depends also on the elastic constants of the crystal. At any given temperature, the less "stiff" the crystal, the greater the vibration amplitude u. This means that u is much greater at any one temperature for a soft, low-melting-point metal like lead than it is for, say, tungsten. Substances with low melting points have quite large values of u even at room temperature and therefore yield rather poor back-reflection photographs. For example, thermal atomic vibration in lead at 20°C reduces the intensity of the highest-angle line observed with Cu $K\alpha$ radiation (at about 161° 2θ) to only 18 percent ($e^{-2M} = 0.18$) of the value for atoms at rest.

In only one application described in this book (Sec. 14–10) will we need any quantitative information about the temperature factor e^{-2M}, but it is convenient to describe the calculation here. Formally, we allow for the effect by defining f as the atomic scattering factor of an atom undergoing thermal vibration, f_0 as the same quantity for an atom at rest, and relating the two by

$$f = f_0 e^{-M}.$$

(The quantity f_0 is then the scattering factor as usually tabulated, for example in Appendix 12.) Because the intensity of any line depends on f^2, calculated intensities must be multiplied by e^{-2M} to allow for thermal vibration. The quantity M depends on both the amplitude u of thermal vibration and the scattering angle 2θ:

$$M = 2\pi^2 \left(\frac{\overline{u^2}}{d^2}\right) = 8\pi^2 \overline{u^2} \left(\frac{\sin\theta}{\lambda}\right)^2 = B\left(\frac{\sin\theta}{\lambda}\right)^2 \qquad (4\text{–}17)$$

where $\overline{u^2}$ is the mean square displacement of the atom in a direction normal to the reflecting planes. The exact calculation of $\overline{u^2}$ as a function of temperature is extremely difficult, which means that M or B is hard to determine accurately. Debye has given the following expression:

$$M = \frac{6h^2T}{mk\Theta^2}\left[\phi(x) + \frac{x}{4}\right]\left(\frac{\sin\theta}{\lambda}\right)^2, \qquad (4\text{–}18)$$

where h is Planck's constant, T the absolute temperature, m the mass of the vibrating atom, k Boltzmann's constant, Θ the Debye characteristic temperature of the substance

in °K, $x = \Theta/T$, and $\phi(x)$ is a function tabulated, along with values of Θ, in Appendix 15. Because $m = A/N$, where A = atomic weight and N = Avogadro's number, the coefficient of the bracketed terms above becomes

$$\frac{6h^2T}{mk\Theta^2} = \frac{(6)(6.02 \times 10^{26})(6.63 \times 10^{-34})^2T}{A\Theta^2(1.38 \times 10^{-23})(10^{-20})} = \frac{1.15 \times 10^4T}{A\Theta^2}$$

if λ is in angstroms. Equation (4–18) is approximate and applies only to elements with cubic crystal structure.

For thorough treatments of the effect of thermal vibration on the diffraction pattern, see James [G.7] and Warren [G.30].

The thermal vibration of atoms has another effect on diffraction patterns. Besides decreasing the intensity of diffraction lines, it causes some general coherent scattering in all directions. This is called *temperature-diffuse scattering*; it contributes only to the general background of the pattern and its intensity gradually increases with 2θ. Contrast between lines and background naturally suffers, so this effect is a very undesirable one, leading in extreme cases to diffraction lines in the back-reflection region scarcely distinguishable from the background. Figure 4–21 illustrates this effect. In (a) is shown an extremely hypothetical pattern (only three lines, equally spaced, equally strong, with no background whatever) for atoms at rest; in (b) the lines, decreased in intensity by the factor e^{-2M}, are superimposed on a background of thermal diffuse scattering.

In the phenomenon of temperature-diffuse scattering we have another example, beyond those alluded to in Sec. 3–7, of scattering at non-Bragg angles. Here again it is not surprising that such scattering should occur, since the displacement of atoms from their mean positions constitutes a kind of crystal imperfection and leads to a partial breakdown of the conditions necessary for perfect destructive interference between rays scattered at non-Bragg angles.

The effect of thermal vibration also illustrates what has been called "the approximate law of conservation of diffracted energy." This law states that the total energy diffracted by a particular specimen under particular experimental conditions is roughly constant. Therefore, anything done to alter the physical condition of the specimen does not alter the total amount of diffracted energy but

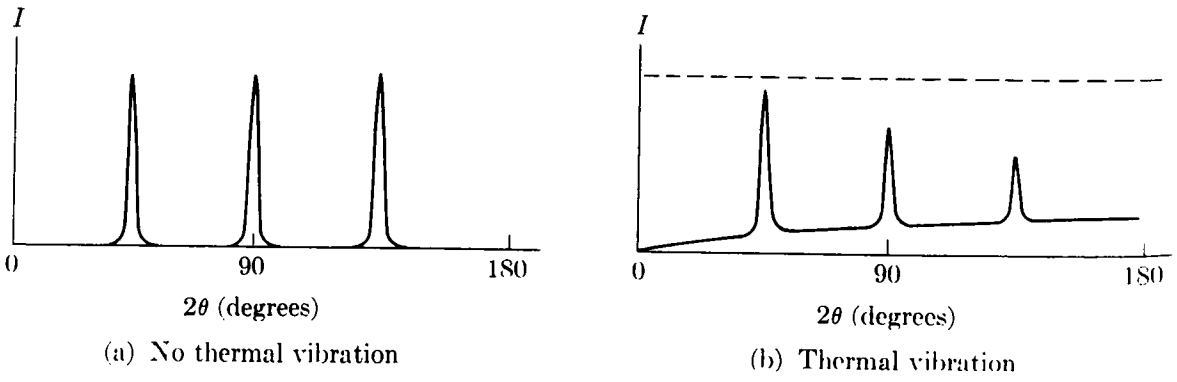

Fig. 4–21 Effect of thermal vibration of the atoms on a powder pattern. Very schematic, see text.

The agreement obtained here between observed and calculated intensities is satisfactory. Note how the value of the multiplicity p exerts a strong control over the line intensity. The values of $|F|^2$ and of the Lorentz-polarization factor vary smoothly with θ, but the values of p, and therefore of I, vary quite irregularly.

A more complicated structure may now be considered, namely that of the zinc-blende form of ZnS, shown in Fig. 2–19(b). This form of ZnS is cubic and has a lattice parameter of 5.41 Å. We will calculate the relative intensities of the first six lines on a Debye–Scherrer pattern made with Cu $K\alpha$ radiation.

As always, the first step is to work out the structure factor. ZnS has four zinc and four sulfur atoms per unit cell, located in the following positions:

$$\text{Zn: } \tfrac{1}{4}\ \tfrac{1}{4}\ \tfrac{1}{4} + \text{face-centering translations,}$$

$$\text{S: } 0\ 0\ 0 + \text{face-centering translations.}$$

Since the structure is face-centered, we know that the structure factor will be zero for planes of mixed indices. We also know, from example (e) of Sec. 4–6, that the terms in the structure-factor equation corresponding to the face-centering translations can be factored out and the equation for unmixed indices written down at once:

$$F = 4[f_S + f_{Zn}e^{(\pi i/2)(h+k+l)}].$$

$|F|^2$ is obtained by multiplication of the above by its complex conjugate:

$$|F|^2 = 16[f_S + f_{Zn}e^{(\pi i/2)(h+k+l)}][f_S + f_{Zn}e^{-(\pi i/2)(h+k+l)}].$$

This equation reduces to the following form:

$$|F|^2 = 16\left[f_S^2 + f_{Zn}^2 + 2f_S f_{Zn}\cos\frac{\pi}{2}(h + k + l)\right].$$

Further simplification is possible for various special cases:

$$|F|^2 = 16(f_S^2 + f_{Zn}^2) \qquad \text{when } (h + k + l) \text{ is odd;} \tag{4–22}$$

$$|F|^2 = 16(f_S - f_{Zn})^2 \qquad \text{when } (h + k + l) \text{ is an odd multiple of 2;} \tag{4–23}$$

$$|F|^2 = 16(f_S + f_{Zn})^2 \qquad \text{when } (h + k + l) \text{ is an even multiple of 2.} \tag{4–24}$$

The intensity calculations are carried out in Table 4–3, with some columns omitted for the sake of brevity.

Remarks

Columns 5 and 6: These values are read from scattering-factor curves plotted from the data of Appendix 12.

Column 7: $|F|^2$ is obtained by the use of Eq. (4–22), (4–23), or (4–24), depending on the particular values of *hkl* involved. Thus, Eq. (4–22) is used for the 111 reflection and Eq. (4–24) for the 220 reflection.

Columns 10 and 11: The agreement obtained here between calculated and observed intensities is again satisfactory. In this case, both the values of $|F|^2$ and of p vary irregularly with θ, leading to an irregular variation of I.

One further remark on intensity calculations is necessary. In the powder method, two sets of planes with different Miller indices can reflect to the same

only its distribution in space. This "law" is not at all rigorous, but it does prove helpful in considering many diffraction phenomena. For example, at low temperatures there is very little background scattering due to thermal agitation and the diffraction lines are relatively intense; if the specimen is now heated to a high temperature, the lines will become quite weak and the energy which is lost from the lines will appear in a spread-out form as temperature-diffuse scattering.

4–12 INTENSITIES OF POWDER PATTERN LINES

We are now in a position to gather together the factors discussed in preceding sections into an equation for the relative intensity of powder pattern lines.

Debye–Scherrer Camera

$$\text{(Approximate)} \qquad \boxed{I = |F|^2 p \left(\frac{1 + \cos^2 2\theta}{\sin^2 \theta \cos \theta}\right)}, \qquad (4\text{–}19)$$

where I = relative integrated intensity (arbitrary units), F = structure factor, p = multiplicity factor, and θ = Bragg angle. The trigonometric terms in parentheses are the Lorentz-polarization factor. In arriving at this equation, we have omitted factors which are constant for all lines of the pattern. For example, all that is retained of the Thomson equation (Eq. 4–2) is the polarization factor $(1 + \cos^2 2\theta)$, with constant factors, such as the intensity of the incident beam and the charge and mass of the electron, omitted. The intensity of a diffraction line is also directly proportional to the irradiated volume of the specimen and inversely proportional to the camera radius, but these factors are again constant for all diffraction lines and may be neglected. Omission of the temperature and absorption factors means that Eq. (4–19) is valid only for lines fairly close together on the pattern; this latter restriction is not as serious as it may sound. Finally, it should be remembered that this equation gives the relative *integrated* intensity, i.e., the relative area under the curve of intensity vs. 2θ.

If an exact expression is required, the absorption factor $A(\theta)$ and the temperature factor e^{-2M} must be inserted:

$$\text{(Exact)} \qquad I = |F|^2 p \left(\frac{1 + \cos^2 2\theta}{\sin^2 \theta \cos \theta}\right) A(\theta) e^{-2M}. \qquad (4\text{–}20)$$

Diffractometer

Here the absorption factor is independent of θ and so does not enter into the calculation of relative intensities. Equation (4–19) becomes still less precise, because there is no longer any approximate cancellation of the absorption and temperature factors. Equation (4–19) may still be used, for adjacent lines on the pattern, but the calculated intensity of the higher-angle line, relative to that of the lower-angle line, will always be somewhat too large because of the omission of the temperature factor.

The exact equation for the diffractometer is

$$\text{(Exact)} \qquad I = |F|^2 p \left(\frac{1 + \cos^2 2\theta}{\sin^2 \theta \cos \theta}\right) e^{-2M}. \qquad (4\text{–}21)$$

Qualifications

The two following effects can make the above intensity equations invalid:

1) *Preferred orientation.* From the way in which the cos θ portion of the Lorentz factor was determined in Sec. 4–9, it follows that Eqs. (4–19) through (4–21) are valid only when the crystals making up the specimen are randomly oriented in space. Preferred orientation of the crystal grains causes radical disagreement between calculated and observed intensities and, when such disagreement exists, preferred orientation should be the first possible cause to be suspected. It is relatively easy to prepare powder-compact specimens from ground powders or metal filings so that the ideal of perfect randomness of orientation is closely approached, but virtually all polycrystalline specimens of metal wire, metal sheet, manufactured ceramics, and even natural rocks or minerals will exhibit more or less preferential orientation of the grains.

2) *Extinction* [G.7, G.30]. As mentioned in Sec. 3–7, all real crystals are imperfect, in the sense that they have a mosaic structure, and the degree of imperfection can vary greatly from one crystal to another. Equations (4–19) through (4–21) are derived on the basis of the so-called "ideally imperfect" crystal, one in which the mosaic blocks are quite small (of the order of 10^{-4} cm to 10^{-5} cm in thickness) and so disoriented that they are all essentially nonparallel. Such a crystal has maximum reflecting power. A crystal made up of large mosaic blocks, some or all of which are accurately parallel to one another, is more nearly perfect and has a lower reflecting power. This *decrease* in the integrated intensity of the diffracted beam as the crystal becomes more nearly perfect is called *extinction.* Extinction is absent for the ideally imperfect crystal, and the presence of extinction invalidates Eqs. (4–19) through (4–21). Any treatment that will make a crystal more imperfect will reduce extinction and, for this reason alone, powder specimens should be ground as fine as possible. Grinding not only reduces the crystal size but also tends to decrease the mosaic block size, disorient the mosaic blocks, and strain them nonuniformly. (The theory of the extinction effect is difficult. To prove that imperfections in a crystal increase its reflecting power would take us too far afield, but an experimental proof is given in Sec. 8–7.)

The extinction effect can operate, not only in single-crystal specimens, but also in the individual grains of polycrystalline specimens. Extinction may be assumed to be absent in ground or filed powders and is usually negligible in fine-grained polycrystalline specimens. If its presence is suspected in the latter, the specimen can always be reduced to powder by grinding or filing.

4–13 EXAMPLES OF INTENSITY CALCULATIONS

The use of Eq. (4–19) will be illustrated by the calculation of the position and relative intensities of the diffraction lines on a Debye–Scherrer pattern of copper, made with Cu $K\alpha$ radiation. The calculations are most readily carried out in tabular form, as in Table 4–2.

Remarks

Column 2: Since copper is face-centered cubic, F is equal to $4f_{Cu}$ for lines of unmixed indices and zero for lines of mixed indices. The reflecting plane indices, all unmixed, are

Table 4–2

1	2	3	4	5	6	7	8
Line	*hkl*	$h^2 + k^2 + l^2$	$\sin^2\theta$	$\sin\theta$	θ	$\frac{\sin\theta}{\lambda}$ (Å^{-1})	f_{Cu}
1	111	3	0.1365	0.369	21.7°	0.24	22.1
2	200	4	0.1820	0.427	25.3	0.27	20.9
3	220	8	0.364	0.603	37.1	0.39	16.8
4	311	11	0.500	0.707	45.0	0.46	14.8
5	222	12	0.546	0.739	47.6	0.48	14.2
6	400	16	0.728	0.853	58.5	0.55	12.5
7	331	19	0.865	0.930	68.4	0.60	11.5
8	420	20	0.910	0.954	72.6	0.62	11.1

1	9	10	11	12	13	14
Line	F^2	p	$\frac{1+\cos^2 2\theta}{\sin^2\theta\cos\theta}$	Relative integrated intensity		
				Calc.	Calc.	Obs.
1	7810	8	12.03	7.52×10^5	10.0	vs
2	6990	6	8.50	3.56	4.7	s
3	4520	12	3.70	2.01	2.7	s
4	3500	24	2.83	2.38	3.2	s
5	3230	8	2.74	0.71	0.9	m
6	2500	6	3.18	0.48	0.6	w
7	2120	24	4.81	2.45	3.3	s
8	1970	24	6.15	2.91	3.9	s

written down in this column in order of increasing values of $(h^2 + k^2 + l^2)$, from Appendix 10.

Column 4: For a cubic crystal, values of $\sin^2\theta$ are given by Eq. (3–10):

$$\sin^2\theta = \frac{\lambda^2}{4a^2}(h^2 + k^2 + l^2).$$

In this case, $\lambda = 1.542$ Å (Cu $K\alpha$) and $a = 3.615$ Å (lattice parameter of copper). Therefore, multiplication of the integers in column 3 by $\lambda^2/4a^2 = 0.0455$ gives the values of $\sin^2\theta$ listed in column 4. In this and similar calculations, three-figure accuracy is ample.

Column 6: Needed to determine the Lorentz-polarization factor and $(\sin\theta)/\lambda$.

Column 7: Obtained from Appendix 11. Needed to determine f_{Cu}.

Column 8: Obtained from Appendix 12.

Column 9: Obtained from the relation $F^2 = 16f_{Cu}^2$.

Column 10: Obtained from Appendix 13.

Column 11: Obtained from Appendix 14.

Column 12: These values are the product of the values in columns 9, 10, and 11, according to Eq. (4–19).

Column 13: Values from column 12 recalculated to give the first line an arbitrary intensity of 10, i.e., "normalized" to 10 for the first line.

Column 14: These entries give the observed intensities, visually estimated according to the following simple scale, from the original film for copper in Fig. 3–13 (vs = very strong, s = strong, m = medium, w = weak).

The agreement obtained here between observed and calculated intensities is satisfactory. Note how the value of the multiplicity p exerts a strong control over the line intensity. The values of $|F|^2$ and of the Lorentz-polarization factor vary smoothly with θ, but the values of p, and therefore of I, vary quite irregularly.

A more complicated structure may now be considered, namely that of the zinc-blende form of ZnS, shown in Fig. 2–19(b). This form of ZnS is cubic and has a lattice parameter of 5.41 Å. We will calculate the relative intensities of the first six lines on a Debye–Scherrer pattern made with Cu $K\alpha$ radiation.

As always, the first step is to work out the structure factor. ZnS has four zinc and four sulfur atoms per unit cell, located in the following positions:

$$\text{Zn: } \tfrac{1}{4}\,\tfrac{1}{4}\,\tfrac{1}{4} + \text{face-centering translations,}$$

$$\text{S: } 0\,0\,0 + \text{face-centering translations.}$$

Since the structure is face-centered, we know that the structure factor will be zero for planes of mixed indices. We also know, from example (e) of Sec. 4–6, that the terms in the structure-factor equation corresponding to the face-centering translations can be factored out and the equation for unmixed indices written down at once:

$$F = 4[f_S + f_{Zn}e^{(\pi i/2)(h+k+l)}].$$

$|F|^2$ is obtained by multiplication of the above by its complex conjugate:

$$|F|^2 = 16[f_S + f_{Zn}e^{(\pi i/2)(h+k+l)}][f_S + f_{Zn}e^{-(\pi i/2)(h+k+l)}].$$

This equation reduces to the following form:

$$|F|^2 = 16\left[f_S^2 + f_{Zn}^2 + 2f_S f_{Zn}\cos\frac{\pi}{2}(h + k + l)\right].$$

Further simplification is possible for various special cases:

$$|F|^2 = 16(f_S^2 + f_{Zn}^2) \qquad \text{when } (h + k + l) \text{ is odd;} \tag{4–22}$$

$$|F|^2 = 16(f_S - f_{Zn})^2 \qquad \text{when } (h + k + l) \text{ is an odd multiple of 2;} \tag{4–23}$$

$$|F|^2 = 16(f_S + f_{Zn})^2 \qquad \text{when } (h + k + l) \text{ is an even multiple of 2.} \tag{4–24}$$

The intensity calculations are carried out in Table 4–3, with some columns omitted for the sake of brevity.

Remarks

Columns 5 and 6: These values are read from scattering-factor curves plotted from the data of Appendix 12.

Column 7: $|F|^2$ is obtained by the use of Eq. (4–22), (4–23), or (4–24), depending on the particular values of *hkl* involved. Thus, Eq. (4–22) is used for the 111 reflection and Eq. (4–24) for the 220 reflection.

Columns 10 and 11: The agreement obtained here between calculated and observed intensities is again satisfactory. In this case, both the values of $|F|^2$ and of p vary irregularly with θ, leading to an irregular variation of I.

One further remark on intensity calculations is necessary. In the powder method, two sets of planes with different Miller indices can reflect to the same